

3 Black Holes

3.1 Concept Questions

1. What evidence do astronomers currently accept as indicating the presence of a black hole in a system?
2. Why can astronomers measure the masses of supermassive black holes only in relatively nearby galaxies?
3. To what extent (with what accuracy) are real black holes in our Universe described by the no-hair theorem?
4. Does the no-hair theorem apply inside a black hole?
5. Black holes lose their hair on a light-crossing time. How long is a light-crossing time for a typical stellar-sized or supermassive astronomical black hole?
6. Relativists say that the metric is $g_{\mu\nu}$, but they also say that the metric is $ds^2 = g_{\mu\nu} dx^\mu dx^\nu$. How can both statements be correct?
7. The Schwarzschild geometry is said to describe the geometry of spacetime outside the surface of the Sun or Earth. But the Schwarzschild geometry supposedly describes non-rotating masses, whereas the Sun and Earth are rotating. If you collapsed the Sun or Earth to a black hole conserving their mass M and angular momentum L , what would the spin parameter $a = L/M$ relative to the maximum possible for a Kerr black hole?
8. What happens at the horizon of a black hole?
9. As cold matter becomes denser, it goes through the stages of being solid/liquid like a planet, then electron degenerate like a white dwarf, then neutron degenerate like a neutron star, then finally it collapses to a black hole. Why could there not be a denser state of matter, denser than a neutron star, that brings a star to rest inside its horizon?
10. How can an observer determine whether they are “at rest” in the Schwarzschild geometry?
11. An observer outside the horizon of a black hole never sees anything pass through the horizon, even to the end of the Universe. Does the black hole then ever actually collapse, if no one ever sees it do so?
12. If nothing can ever get out of a black hole, how does its gravity get out?
13. Why did Einstein believe that black holes could not exist in nature?
14. In what sense is a rotating black hole “stationary”?

15. What is a white hole? Do they exist?
16. Could the expanding Universe be a white hole?
17. Could the Universe be the interior of a black hole?
18. You know the Schwarzschild metric for a black hole. What is the corresponding metric for a white hole?
19. What is the best kind of black hole to fall into if you want to avoid being tidally torn apart?
20. Why do astronomers often assume that the inner edge of an accretion disk around a black hole occurs at the innermost stable orbit?
21. A collapsing star of uniform density has the geometry of a collapsing Friedmann-Robertson-Walker cosmology. If a spatially flat FRW cosmology corresponds to a star that starts from zero velocity at infinity, then to what do open or closed FRW cosmologies correspond?
22. Is the singularity of a Reissner-Nordström black hole gravitationally attractive or repulsive?
23. If you are a charged particle, which dominates near the singularity of the Reissner-Nordström geometry, the electrical attraction/repulsion or the gravitational attraction/repulsion?
24. Is a white hole gravitationally attractive or repulsive?
25. What happens if you fall into a white hole?
26. Which way does time go in Parallel Universes in the Reissner-Nordström geometry?
27. What does it mean that geodesics inside a black hole can have negative energy?
28. Can geodesics have negative energy outside a black hole? How about inside the ergosphere?
29. Physically, what causes mass inflation?
30. Is mass inflation likely to occur inside real astronomical black holes?
31. What happens at the X point, where the ingoing and outgoing inner horizons of the Reissner-Nordström geometry intersect?
32. Can a particle like an electron or proton, whose charge far exceeds its mass (in Planck units), be modeled as Reissner-Nordström black hole?

33. Does it make sense that a person might be at rest in the Kerr-Newman geometry? How would the Boyer-Linquist coordinates of such a person vary along their worldline?
34. In identifying M as the mass and a the angular momentum per unit mass of the black hole in the Boyer-Linquist metric, why is it sufficient to consider the behavior of the metric at $r \rightarrow \infty$?
35. Does space move faster than light inside the ergosphere?
36. If space moves faster than light inside the ergosphere, why is the outer boundary of the ergosphere not a horizon?
37. Do closed timelike curves make sense?
38. What does Carter's fourth integral of motion Q signify physically?
39. What is special about a principal null congruence?
40. Evaluated in the locally inertial frame of a principal null congruence, the spin-0 component of the Weyl scalar of the Kerr geometry is $C = -M/(r - ia \cos \theta)^3$, which looks like the Weyl scalar $C = -M/r^3$ of the Schwarzschild geometry but with radius r replaced by the complex radius $r - ia \cos \theta$. Is there something deep here? Can the Kerr geometry be constructed from the Schwarzschild geometry by complexifying the radial coordinate r ?

3.2 What's important?

1. Astronomical evidence suggests that stellar-sized and supermassive black holes exist ubiquitously in nature.
2. The no-hair theorem, and when and why it applies.
3. The physical picture of black holes as regions of spacetime where space is falling faster than light.
4. A physical understanding of how the metric of a black hole relates to its physical properties.
5. Penrose (conformal) diagrams. In particular, the Penrose diagrams of the various kinds of vacuum black hole: Schwarzschild, Reissner-Nordström, Kerr-Newman.
6. What really happens inside black holes. Collapse of a star. Mass inflation instability.

3.3 Observational evidence

It is beyond the scope of this course to discuss the observational evidence for black holes in any detail. However, it is useful to summarize a few facts.

1. Observational evidence supports the idea that black holes occur ubiquitously in nature. They are not observed directly, but reveal themselves through their effects on their surroundings. Two kinds of black hole are observed: stellar-sized black holes in x-ray binary systems, mostly in our own Milky Way galaxy, and supermassive black holes in Active Galactic Nuclei (AGN) found at the centers of our own and other galaxies.
2. The primary evidence that astronomers accept as indicating the presence of a black hole is a lot of mass compacted into a tiny space.
 - (a) In an x-ray binary system, if the mass of the compact object exceeds $3M_{\odot}$, the maximum theoretical mass of a neutron star, then the object is considered to be a black hole. Many hundreds of x-ray binary systems are known in our Milky Way galaxy, but only 10s of these have measured masses, and in about 20 the measured mass indicates a black hole.
 - (b) Several tens of thousands of AGN have been cataloged, identified either in the radio, optical, or x-rays. But only in nearby galaxies can the mass of a supermassive black hole be measured directly. This is because it is only in nearby galaxies that the velocities of gas or stars can be measured sufficiently close to the nuclear center to distinguish a regime where the velocity becomes constant, so that the mass can be attribute to an unresolved central point as opposed to a continuous distribution of stars. The masses of about 40 supermassive black holes have been measured in this way. The masses range from the $4 \times 10^6 M_{\odot}$ mass of the black hole at the center of the Milky Way to the $3 \times 10^9 M_{\odot}$ mass of the black hole at the center of the M87 galaxy at the center of the Virgo cluster at the center of the Local Supercluster of galaxies.
3. Secondary evidences for the presence of a black hole are:
 - (a) high luminosity;
 - (b) non-stellar spectrum, extending from radio to gamma-rays;
 - (c) rapid variability.
 - (d) relativistic jets.

Jets in AGN are often one-sided, and a few that are bright enough to be resolved at high angular resolution show superluminal motion. Both evidences indicate that jets are commonly relativistic, moving at close to the speed of light. There are a few cases of jets in x-ray binary systems.

4. Stellar-sized black holes are thought to be created in supernovae as the result of the core-collapse of stars more massive than about $25 M_{\odot}$ (this number depends in part on uncertain computer simulations). Supermassive black holes are probably created initially in the same way, but they then grow by accretion of gas funneled to the center of the galaxy. The growth rates inferred from AGN luminosities are consistent with this picture.

5. Long gamma-ray bursts (lasting more than about 2 seconds) are associated observationally with supernovae. It is thought that in such bursts we are seeing the formation of a black hole. As the black hole gulps down the huge quantity of material needed to make it, it regurgitates a relativistic jet that punches through the envelope of the star. If the jet happens to be pointed in our direction, then we see it relativistically beamed as a gamma-ray burst.
6. Astronomical black holes present the only realistic prospect for testing general relativity in the strong field regime, since such fields cannot be reproduced in the laboratory. At the present time the observational tests of general relativity from astronomical black holes are at best tentative. One test is the redshifting of 7 keV iron lines in a small number of AGN, notably MCG-6-30-15, which can be interpreted as being emitted by matter falling on to a rotating (Kerr) black hole.
7. At present, no gravitational waves have been definitely detected from anything. In the future, gravitational wave astronomy should eventually detect the merger of two black holes. If the waveforms of merging black holes are consistent with the predictions of general relativity, it will provide a far more stringent test of strong field general relativity than has been possible to date.
8. Although gravitational waves have yet to be detected directly, their existence has been inferred from the gradual speeding up of the orbit of the Hulse-Taylor binary, which consists of two neutron stars, one of which PSR1913+16 is a pulsar. The parameters of the orbit have been measured with exquisite precision, and the rate of orbital speed-up is in good agreement with the energy loss by quadrupole gravitational wave emission predicted by general relativity.

3.4 No-hair theorem

I will state and justify the no-hair theorem, but I will not prove it mathematically, since the proof is technical.

The **no-hair** theorem states that a stationary black hole in asymptotically flat space is characterized by just three quantities:

1. Mass M ;
2. Electric charge Q ;
3. Spin, usually parameterized by the angular momentum a per unit mass.

The mechanism by which a black hole loses its hair is gravitational radiation. When initially formed, whether from the collapse of a massive star or from the merger of two black holes, a black hole will form a complicated, oscillating region of spacetime. But over the course of several light crossing times, the oscillations lose energy by gravitational radiation, and damp out, leaving a stationary black hole.

Real astronomical black holes are not isolated, and continue to accrete (cosmic microwave background photons, if nothing else). However, the timescale (a light crossing time) for oscillations to damp out by gravitational radiation is usually far shorter than the timescale

for accretion, so in practice real black holes are extremely well described by no-hair solutions almost all of their lives.

The physical reason that the no-hair theorem applies is that space is falling faster than light inside the horizon. Consequently, unlike a star, no energy can bubble up from below to replace the energy lost by gravitational radiation, so that the black hole tends to the lowest energy state characterized by conserved quantities.

As a corollary, the no-hair theorem does not apply from the inner horizon of a black hole inward, because there space ceases to fall superluminally.

If there exist other absolutely conserved quantities, such as magnetic charge (magnetic monopoles), or various supersymmetric charges in theories where supersymmetry is not broken, then the black hole will also be characterized by those quantities.

Black holes are expected not to conserve quantities such as baryon or lepton number that are thought not to be absolutely conserved, even though they appear to be conserved in low energy physics.

Other solutions exist that describe black holes in spacetimes that are not asymptotically flat, such as spacetimes with a cosmological constant.

It is legitimate to think of the process of reaching a stationary state as analogous to reaching a condition of thermodynamic equilibrium, in which a macroscopic system is described by a small number of parameters associated with the conserved quantities of the system.

3.5 Schwarzschild geometry

The Schwarzschild geometry was discovered by Karl Schwarzschild in late 1915 at essentially the same time that Einstein was arriving at his final version of the General Theory of Relativity.

3.5.1 Schwarzschild metric

The **Schwarzschild metric** (units $c = G = 1$) is, in a polar coordinate system $\{t, r, \theta, \phi\}$,

$$ds^2 = \left(1 - \frac{2M}{r}\right) dt^2 - \left(1 - \frac{2M}{r}\right)^{-1} dr^2 - r^2 d\sigma^2 \quad (1)$$

where $d\sigma^2$ (this is the Landau & Lifshitz notation) is the metric of a unit 2-sphere

$$d\sigma^2 = d\theta^2 + \sin^2\theta d\phi^2 . \quad (2)$$

The Schwarzschild geometry describes the simplest kind of black hole: a black hole with mass M , but no electric charge, and no spin.

The geometry describes not only a black hole, but also any empty space surrounding a spherically symmetric mass. Thus the Schwarzschild geometry describes to a good approximation the spacetime outside the surfaces of the Sun and the Earth.

Comparison with the spherically symmetric Newtonian metric

$$ds^2 = (1 + 2\Phi)dt^2 - (1 - 2\Phi)(dr^2 + r^2 d\theta^2) \quad (3)$$

with Newtonian potential

$$\Phi(r) = -\frac{M}{r} \quad (4)$$

establishes that the M in the Schwarzschild metric is to be interpreted as the mass of the black hole.

The Schwarzschild geometry is asymptotically flat, because the metric tends to the Minkowski metric in polar coordinates at large radius

$$ds^2 \rightarrow dt^2 - dr^2 - r^2 d\theta^2 \quad \text{as } r \rightarrow \infty . \quad (5)$$

3.5.2 Birkhoff's theorem

Birkhoff's theorem states that the geometry of empty space surrounding a spherically symmetric matter distribution is the Schwarzschild geometry. That is, if the metric is of the form

$$ds^2 = A(t, r) dt^2 + B(t, r) dt dr + C(t, r) dr^2 + D(t, r) d\theta^2 \quad (6)$$

where the metric coefficients A , B , C , and D are allowed to be arbitrary functions of t and r , and if the energy momentum tensor vanishes, $T_{\mu\nu} = 0$, outside some value of the circumferential radius r' defined by $r'^2 = D$, then the geometry is necessarily Schwarzschild outside that radius.

This means that if a mass undergoes spherically symmetric pulsations, then those pulsations do not affect the geometry of the surrounding spacetime. This reflects the fact that there are no spherically symmetric gravitational waves.

3.5.3 Stationary, static

The Schwarzschild geometry is **stationary**. A spacetime is said to be stationary if and only if there exists a timelike coordinate t such that the metric is independent of t . In other words, the spacetime possesses time translation symmetry: the metric is unchanged by a time translation $t \rightarrow t + t_0$ where t_0 is some constant. Evidently the Schwarzschild metric (1) is independent of the timelike coordinate t , and is therefore stationary, time translation symmetric.

The Schwarzschild geometry is also **static**. A spacetime is static if and only if the coordinates can be chosen so that, in addition to being stationary with respect to a time coordinate t , the spatial coordinates do not change when you move along the tangent vector \mathbf{g}_t . This requires that the tangent vector \mathbf{g}_t be orthogonal to all the spatial tangent vectors

$$\mathbf{g}_t \cdot \mathbf{g}_\mu = g_{t\mu} = 0 \quad \text{for } \mu \neq t . \quad (7)$$

The Gullstrand-Painlevé metric for the Schwarzschild geometry, discussed in section 3.6, is an example of a metric that is stationary but not static (although the underlying spacetime, being Schwarzschild, is static). The Gullstrand-Painlevé metric is independent of the free-fall time t_{ff} , so is stationary, but observers who follow the tangent vector $\mathbf{g}_{t_{\text{ff}}}$ fall into the black hole, so the metric is not manifestly static.

The Schwarzschild time coordinate t is thus identified as a special one: it is the unique time coordinate with respect to which the Schwarzschild geometry is manifestly static.

3.5.4 Spherically symmetric

The Schwarzschild geometry is also **spherically symmetric**. This is evident from the fact that the angular part $r^2 d\Omega^2$ of the metric is the metric of a 2-sphere of radius r . This can be seen as follows. Consider the metric of ordinary flat 3-dimensional Euclidean space in Cartesian coordinates $\{x, y, z\}$:

$$ds^2 = dx^2 + dy^2 + dz^2 . \quad (8)$$

Convert to polar coordinates $\{r, \theta, \phi\}$, defined so that

$$\begin{aligned} x &= r \sin \theta \cos \phi , \\ y &= r \sin \theta \sin \phi , \\ z &= r \cos \theta . \end{aligned} \quad (9)$$

Substituting equations (9) into the Euclidean metric (8) gives

$$ds^2 = dr^2 + r^2(d\theta^2 + \sin^2\theta d\phi^2) . \quad (10)$$

Restricting to a surface $r = \text{constant}$ of constant radius then gives the metric of a 2-sphere of radius r

$$ds^2 = r^2(d\theta^2 + \sin^2\theta d\phi^2) \quad (11)$$

as claimed.

The radius r in Schwarzschild coordinates is the **circumferential radius**, defined such that the proper circumference of the 2-sphere measured by observers at rest in Schwarzschild coordinates is $2\pi r$. This is a coordinate-invariant definition of the meaning of r , which implies that r is a scalar.

3.5.5 Horizon

The **horizon** of the Schwarzschild geometry lies at the Schwarzschild radius $r = r_s$

$$\boxed{r_s = \frac{2GM}{c^2}} . \quad (12)$$

where units of c and G have been restored. Where does this come from? The Schwarzschild metric shows that the scalar spacetime distance squared ds^2 along an interval at rest in

Schwarzschild coordinates, $dr = d\theta = d\phi = 0$, is timelike, lightlike, or spacelike depending on whether the radius is greater than, equal to, or less than $r = 2M$:

$$ds^2 = \left(1 - \frac{2M}{r}\right) dt^2 \quad \begin{cases} > 0 & \text{if } r > 2M, \\ = 0 & \text{if } r = 2M, \\ < 0 & \text{if } r < 2M. \end{cases} \quad (13)$$

Since the worldline of a massive observer must be timelike, it follows that a massive observer can remain at rest only outside the horizon, $r > 2M$. An object at rest at the horizon, $r = 2M$, follows a null geodesic, which is to say it is a possible worldline of a massless particle, a photon. Inside the horizon, $r < 2M$, neither massive nor massless objects can remain at rest.

A full treatment of what is going on requires solving the geodesic equation in the Schwarzschild geometry, but the results may be anticipated already at this point. In effect, space is falling into the black hole. Outside the horizon, space is falling less than the speed of light; at the horizon space is falling at the speed of light; and inside the horizon, space is falling faster than light, carrying everything with it. This is why light cannot escape from a black hole: inside the horizon, space falls inward faster than light, carrying light inward even if that light is pointed radially outward. The statement that space is falling superluminally inside the horizon of a black hole is a coordinate-invariant statement: massive or massless particles are carried inward whatever their state of motion and whatever the coordinate system.

Whereas an interval of coordinate time t switches from timelike outside the horizon to spacelike inside the horizon, an interval of coordinate radius r does the opposite: it switches from spacelike to timelike:

$$ds^2 = - \left(1 - \frac{2M}{r}\right)^{-1} dr^2 \quad \begin{cases} < 0 & \text{if } r > 2M, \\ = 0 & \text{if } r = 2M, \\ > 0 & \text{if } r < 2M. \end{cases} \quad (14)$$

It appears then that the Schwarzschild time and radial coordinates swap roles inside the horizon. Inside the horizon, the radial coordinate becomes timelike, meaning that it becomes a possible worldline of a massive observer. That is, a trajectory at fixed t and decreasing r is a possible worldline. Again this reflects the fact that space is falling faster than light inside the horizon. A person inside the horizon is inevitably compelled as time goes by to move to smaller radial coordinate r .

3.5.6 Proper time

The proper time experienced by an observer at rest in Schwarzschild coordinates, $dr = d\theta = d\phi = 0$, is

$$d\tau = \sqrt{ds^2} = \left(1 - \frac{2M}{r}\right)^{1/2} dt. \quad (15)$$

For an observer at rest at infinity, $r \rightarrow \infty$, the proper time is the same as the coordinate time,

$$d\tau \rightarrow dt \quad \text{as } r \rightarrow \infty. \quad (16)$$

Among other things, this implies that the Schwarzschild time coordinate t is a scalar: not only is it the unique coordinate with respect to which the metric is manifestly static, but it coincides with the proper time of observers at rest at infinity. This coordinate-invariant definition of time t implies that it is a scalar.

At finite radii outside the horizon, $r > 2M$, the proper time $d\tau$ is less than the Schwarzschild time dt , so the clocks of observers at rest run slower at smaller than at larger radii.

At the horizon, $r = 2M$, the proper time $d\tau$ of an observer at rest goes to zero

$$d\tau \rightarrow 0 \quad \text{as } r \rightarrow 2M . \quad (17)$$

This reflects the fact that an object at rest at the horizon is following a null geodesic, and as such experiences zero proper time.

3.5.7 Redshift

An observer at rest at infinity looking through a telescope at an emitter at rest at radius r sees the emitter redshifted by a factor

$$1 + z \equiv \frac{\lambda_{\text{obs}}}{\lambda_{\text{emit}}} = \frac{\nu_{\text{emit}}}{\nu_{\text{obs}}} = \frac{d\tau_{\text{obs}}}{d\tau_{\text{emit}}} = \left(1 - \frac{2M}{r}\right)^{-1/2} . \quad (18)$$

This is an example of the universally valid statement that photons are good clocks: the redshift factor is given by the rate at which the emitter's clock appears to tick relative to the observer's own clock.

It should be emphasized that the redshift factor (18) is valid only for an observer and an emitter at rest in the Schwarzschild geometry. If the observer and emitter are not at rest, then additional special relativistic factors will fold into the redshift.

The redshift goes to infinity for an emitter at the horizon

$$1 + z \rightarrow \infty \quad \text{as } r \rightarrow 2M . \quad (19)$$

Here the redshift tends to infinity regardless of the motion of the observer or emitter. An observer watching an emitter fall through the horizon will see the emitter appear to freeze at the horizon, becoming ever slower and more redshifted. Physically, photons emitted vertically upward at the horizon by an emitter falling through it remain at the horizon for ever, taking an infinite time to get out to the outside observer.

3.5.8 Proper distance

The proper radial distance measure by observers at rest in Schwarzschild coordinates, $dr = d\theta = d\phi = 0$, is

$$dl = \sqrt{-ds^2} = \left(1 - \frac{2M}{r}\right)^{-1/2} dr . \quad (20)$$

For an observer at rest at infinity, $r \rightarrow \infty$, an interval of proper radial distance equals an interval of circumferential radial distance, as you might expect for asymptotically flat space

$$dl \rightarrow dr \quad \text{as } r \rightarrow \infty . \quad (21)$$

At the horizon, $r = 2M$, a proper radial interval dl measured by an observer at rest goes to infinity

$$dl \rightarrow \infty \quad \text{as } r \rightarrow 2M . \quad (22)$$

3.5.9 “Schwarzschild singularity”

The apparent singularity in the Schwarzschild metric at the horizon $r = 2M$ is not a real singularity, because it can be removed by a change of coordinates, such as to Gullstrand-Painlevé coordinates (25). Prior to as late as the 1950s, people, including Einstein, thought that the “Schwarzschild singularity” at $r = 2M$ marked the physical boundary of the Schwarzschild spacetime. After all, an outside observer watching stuff fall in never sees anything beyond that boundary.

Schwarzschild’s choice of coordinates was certainly a natural one. It was natural to search for static solutions, and his time coordinate t is the only one with respect to which the metric is manifestly static. The problem is that physically there can be no static observers inside the horizon: they must necessarily fall inward as time passes. The fact that Schwarzschild’s coordinate system shows an apparent singularity at the horizon reflects the fact that the assumption of a static spacetime necessarily breaks down at the horizon, where space is falling at the speed of light.

Does stuff “actually” fall in, even though no outside observer ever sees it happen? Classically, the answer is yes: when a black hole forms, it does actually collapse, and when an observer falls through the horizon, they really do fall through the horizon. The reason that an outside observer sees everything freeze at the horizon is simply a light travel time effect: it takes an infinite time for light to lift off the horizon and make it to the outside world.

Quantum mechanically, the question of what happens inside the horizon is less clear. If black hole evaporation is unitary, as several prominent physicists advocate, then states inside a black hole must be entangled with those outside, much as a quantum superposition of dead and alive Schrödinger cats are entangled. According to this idea, which is called “black hole complementarity”, what happens to a person who falls inside the horizon of a black hole is an alternate quantum reality. The alternate quantum reality is real to the person who falls in, but not part of the quantum experience of the observer who stays outside.

3.5.10 Embedding diagram

An **embedding diagram** is a visual aid to understanding geometry. It is a depiction of a lower dimensional geometry in a higher dimension. A classic example is the illustration of the geometry of a 2-sphere embedded in 3-dimensional space. The 2-sphere has a meaning independent of any embedding in 3 dimensions because the geometry of the 2-sphere can

be measured by 2-dimensional inhabitants of its surface without reference any encompassing 3-dimensional space. Nevertheless, the pictorial representation aids imagination.

Textbooks sometimes illustrate the Schwarzschild geometry with an embedding diagram that shows the spatial geometry at a fixed instant of Schwarzschild time t . The diagram illustrates the stretching of proper distances in the radial direction. I'll let you figure out how to construct this embedding diagram.

It should be emphasized that the embedding diagram of the Schwarzschild geometry at fixed Schwarzschild time t has a limited physical meaning. Fixing the time t means choosing a certain hypersurface through the geometry. Other choices of hypersurface will yield different diagrams. For example, the Gullstrand-Painlevé metric is spatially flat at fixed free-fall time t_{ff} , so in that case the embedding diagram would simply illustrate flat space, with no funny business at the horizon.

3.5.11 Energy-momentum tensor

The energy-momentum tensor of the Schwarzschild geometry is zero, by construction.

3.5.12 Weyl tensor

It turns out that the 10 components of the Weyl tensor, the tidal part of the Riemann tensor, can be decomposed in any locally inertial frame into 5 complex components of spin 0, ± 1 , and ± 2 . In the Schwarzschild metric, all components vanish except the real spin 0 component. This component is a coordinate-invariant scalar, the Weyl scalar C

$$C = -\frac{M}{r^3}. \quad (23)$$

The Weyl scalar, which expresses the presence of tidal forces, goes to infinity at zero radius

$$C \rightarrow \infty \quad \text{as } r \rightarrow 0 \quad (24)$$

signalling the presence of a real singularity at zero radius.

3.6 Gullstrand-Painlevé coordinates

The Gullstrand-Painlevé metric is an alternative metric for the Schwarzschild geometry, discovered independently by Allvar Gullstrand and Paul Painlevé in (1921). It is plausible, though not obvious, from the form of the metric that the metric physically represents space free-falling radially into the black hole at the Newtonian escape velocity. Such an interpretation emerges rigorously from an analysis in the tetrad formalism. Unlike Schwarzschild coordinates, there is no singularity at the horizon in Gullstrand-Painlevé coordinates. It is striking that the mathematics was known long before physical understanding emerged.

The Gullstrand-Painlevé metric is

$$\boxed{ds^2 = dt_{\text{ff}}^2 - (dr - \beta dt_{\text{ff}})^2 - r^2 d\theta^2}. \quad (25)$$

Here β is the Newtonian escape velocity (with a minus sign because space is falling inward)

$$\beta = - \left(\frac{2M}{r} \right)^{1/2} \quad (26)$$

and t_{ff} is the proper time experienced by an object that free falls radially inward from zero velocity at infinity. The free fall time t_{ff} is related to the Schwarzschild time coordinate t by

$$dt_{\text{ff}} = dt - \frac{\beta}{1 - \beta^2} dr \quad (27)$$

which integrates to

$$t_{\text{ff}} = t + 2M \left[2 \left(\frac{r}{2M} \right)^{1/2} + \ln \left| \frac{(r/2M)^{1/2} - 1}{(r/2M)^{1/2} + 1} \right| \right] . \quad (28)$$

The time axis $\mathbf{g}_{t_{\text{ff}}}$ in Gullstrand-Painlevé coordinates is not orthogonal to the radial axis \mathbf{g}_r , but rather is tilted along the radial axis, $\mathbf{g}_{t_{\text{ff}}} \cdot \mathbf{g}_r = g_{t_{\text{ff}}r} = \beta$.

The proper time of a person at rest in Gullstrand-Painlevé coordinates, $dr = d\theta = d\phi = 0$, is

$$d\tau = dt_{\text{ff}} \sqrt{1 - \beta^2} . \quad (29)$$

The horizon occurs where this proper time vanishes, which happens when the infall velocity β is the speed of light

$$|\beta| = 1 . \quad (30)$$

According to equation (26), this happens at $r = 2M$, which is the Schwarzschild radius, as it should be.

3.7 Eddington-Finkelstein coordinates

In Schwarzschild coordinates, radially infalling or outfalling light rays appear never to cross the horizon of the Schwarzschild black hole. This feature of Schwarzschild coordinates contributed to the historical misconception that black holes stopped at their horizons. In 1958, David Finkelstein carried out a trivial transformation of the time coordinate which seemed to show that infalling light rays could indeed pass through the horizon. It turned out that Eddington had already discovered the transformation in 1924, though at that time the physical implications were not grasped. Again, it is striking that the mathematics was in place long before physical understanding.

In Schwarzschild coordinates, light rays that fall radially ($d\theta = d\phi = 0$) inward or outward follow null geodesics

$$ds^2 = \left(1 - \frac{2M}{r} \right) dt^2 - \left(1 - \frac{2M}{r} \right)^{-1} dr^2 = 0 . \quad (31)$$

Radial null geodesics thus follow

$$\frac{dr}{dt} = \pm \left(1 - \frac{2M}{r}\right) \quad (32)$$

in which the \pm sign is $+$ for outfalling, $-$ for infalling rays. Equation (32) shows that $dr/dt \rightarrow 0$ as $r \rightarrow 2M$, suggesting that null rays, whether infalling or outfalling, never cross the horizon. The solution to equation (32) is

$$t = \pm (r + 2M \ln|r - 2M|) \quad (33)$$

which shows that Schwarzschild time t approaches $\pm\infty$ logarithmically as null rays approach the horizon. Finkelstein defined his time coordinate t_F by

$$t_F \equiv t + 2M \ln|r - 2M| \quad (34)$$

which has the property that infalling null rays follow

$$t_F + r = 0 . \quad (35)$$

In other words, on a spacetime diagram in Finkelstein coordinates, radially infalling light rays move at 45° , the same as in special relativistic spacetime diagrams.

3.8 Kruskal-Szekeres coordinates

Since Finkelstein transformed coordinates so that radially infalling light rays moved at 45° in a spacetime diagram, it is natural to look for coordinates in which outfalling as well as infalling light rays are at 45° . Kruskal and Szekeres independently provided such a transformation, in 1960.

Define the tortoise (or Regge-Wheeler 1959) coordinate r^* by

$$r^* \equiv \int \frac{dr}{1 - 2M/r} = r + 2M \ln|r - 2M| . \quad (36)$$

Then radially infalling and outfalling null rays follow

$$\begin{aligned} r^* + t &= 0 \quad \text{infalling} , \\ r^* - t &= 0 \quad \text{outfalling} . \end{aligned} \quad (37)$$

In a spacetime diagram in coordinates t and r^* , infalling and outfalling light rays are indeed at 45° . Unfortunately the metric in these coordinates is still singular at the horizon $r = 2M$:

$$ds^2 = \left(1 - \frac{2M}{r}\right) (dt^2 - dr^{*2}) - r^2 d\phi^2 . \quad (38)$$

The singularity at the horizon can be eliminated by the following transformation into Kruskal-Szekeres coordinates t_K and r_K :

$$\begin{aligned} r_K + t_K &= e^{(r^*+t)/2} , \\ r_K - t_K &= \pm e^{(r^*-t)/2} , \end{aligned} \quad (39)$$

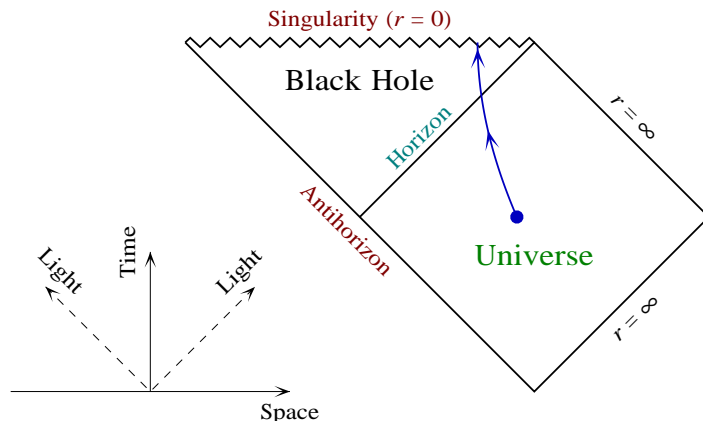


Figure 1: Penrose diagram of the Schwarzschild geometry.

where the \pm sign in the last equation is $+$ outside the horizon, $-$ inside the horizon. The Kruskal-Szekeres metric is

$$ds^2 = r^{-1}e^{-r} (dt_K^2 - dr_K^2) - r^2 d\phi^2 \quad (40)$$

which is non-singular at the horizon. The Schwarzschild radial coordinate r , which appears in the factors $r^{-1}e^{-r}$ and r^2 in the Kruskal metric, is to be understood as an implicit function of the Kruskal coordinates t_K and r_K .

3.9 Penrose diagrams

Roger Penrose, as so often, had a novel take on the business of spacetime diagrams. Penrose conceived that the primary purpose of a spacetime diagram should be to portray the causal structure of the spacetime, and that the specific choice of coordinates was largely irrelevant. After all, general relativity allows arbitrary choices of coordinates.

In addition to requiring that light rays be at 45° , Penrose wanted to bring regions at infinity (in time or space) to a finite position on the spacetime diagram, so that the entire spacetime could be seen at once. He calls these thing conformal diagrams, but the rest of us commonly call them **Penrose diagrams**.

Penrose diagrams are bona-fide spacetime diagrams. For example, a coordinate transformation from Kruskal to “Penrose” coordinates

$$\begin{aligned} r_P + t_P &= \frac{r_K + t_K}{2 + |r_K + t_K|}, \\ r_P - t_P &= \frac{r_K - t_K}{2 - |r_K - t_K|}, \end{aligned} \quad (41)$$

brings spatial and temporal infinity to finite values of the coordinates, while keeping infalling and outfalling light rays at 45° in the spacetime diagram. However, there are many such transformations, and Penrose would be the last person to advocate any one of them in particular.

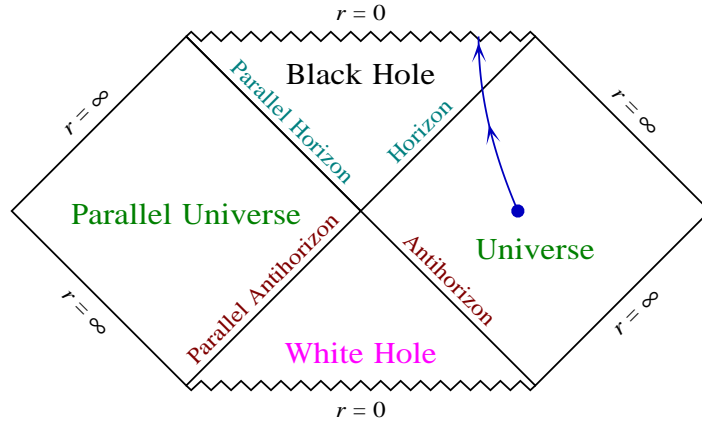


Figure 2: Penrose diagram of the complete, analytically extended Schwarzschild geometry.

3.10 Schwarzschild white hole, wormhole

The Kruskal-Szekeres spacetime diagram reveals a new feature that was not apparent in Schwarzschild or Finkelstein coordinates. Dredged from the depths of $t = -\infty$ appears a null line $r_K + t_K = 0$. The null line is at radius $r = 2M$, but it does not correspond to the horizon that a person might fall into. The null line is called the **antihorizon**. It is also called the past horizon, while the true horizon is called the future horizon.

The Kruskal-Szekeres (= Schwarzschild) geometry is analytic, and there is a unique analytic continuation of the geometry through the antihorizon. The analytic continuation is a time-reversed copy of the original Schwarzschild geometry, glued at the antihorizon. Whereas the original Schwarzschild geometry showed an asymptotically flat region and a black hole region separated by a horizon, the complete analytically extended Schwarzschild geometry shows two asymptotically flat regions, together with a black hole and a white hole. Relativists label the regions I, II, III, and IV, but I like to call them by name: “Universe”, “Black Hole”, “Parallel Universe”, and “White Hole”.

The **white hole** is a time-reversed version of the black hole. Whereas space falls inward faster than light inside the black hole, space falls outward faster than light inside the white hole. In the Gullstrand-Painlevé metric (25), the velocity $\beta = \pm(2M/r)^{1/2}$ is negative for the black hole, positive for the white hole.

The Kruskal or Penrose diagrams show that the universe and the parallel universe are connected, but only by spacelike lines. This spacelike connection is called the **Einstein-Rosen bridge**, and constitutes a wormhole connecting the two universes. Because the connection is spacelike, it is impossible for a traveler to pass through this wormhole.

Although two travelers, one from the universe and one from the parallel universe, cannot travel to each other’s universe, they can meet, but only inside the black hole. Inside the black hole, they can talk to each other, and they can see light from each other’s universe. Sadly, the enlightenment is only temporary, because they are doomed soon to hit the central

singularity.

It should be emphasized that the white hole and the wormhole in the Schwarzschild geometry are a mathematical construction with as far as anyone knows no relevance to reality. Nevertheless it is intriguing that such bizarre objects emerge already in the simplest general relativistic solutions for black holes.

3.11 Collapse to a black hole

Realistic collapse of a star to a black hole is not expected to produce a white hole or parallel universe.

The simplest model of a collapsing star is a spherical ball of uniform density and zero pressure which free falls from zero velocity at infinity. In this simple model, the interior of the star is described by a collapsing Friedmann-Robertson-Walker metric (the canonical cosmological metric), while the exterior is described by the Schwarzschild solution. The assumption that the star collapses from zero velocity at infinity implies that the FRW metric is spatially flat, the simplest case. To continue the geometry between Schwarzschild and FRW metrics, it is neatest to use the Gullstrand-Painlevé metric, with the Gullstrand-Painlevé infall velocity β at the edge of the star set equal to minus r times the Hubble parameter $-rH \equiv -r d \ln a/dt$ of the collapsing FRW metric.

The simple model shows that the antihorizon of the complete Schwarzschild geometry is replaced by the surface of the collapsing star, and that beyond the antihorizon is not a parallel universe and a white hole, but merely the interior of the star (and the distant Universe glimpsed through the star's interior).

Since light can escape from the collapsing star system as long as it is even slightly larger than its Schwarzschild radius, it is possible to take the view that the horizon comes instantaneously into being at the moment the star collapses through its Schwarzschild radius. This definition of the horizon is called the apparent horizon.

Hawking has advocated that a better definition of the horizon is to take it to be the boundary between outgoing null rays that fall into the black hole versus those that go to infinity. In any evolving situation, this definition of the horizon, which is called the absolute horizon, depends formally on what happens in the infinite future, though in slowly evolving systems the absolute horizon can be located with some precision without knowing the future. The absolute horizon of the collapsing star forms before the star has collapsed, and grows to meet the apparent horizon as the star falls through its Schwarzschild radius.

In this simple model, the central singularity forms slightly before the star has collapsed to zero radius. The formation of the singularity is marked by the fact that light rays emitted at zero radius cease to be able to move outward. In other words, the singularity forms when space starts to fall into it faster than light.

3.12 Killing vectors

The Schwarzschild metric presents an opportunity to introduce the concept of **Killing vectors** (after Mr. Killing, not because the vectors kill things, though the latter is true), which are associated with symmetries of the spacetime.

3.12.1 Time translation symmetry

The time translation invariance of the Schwarzschild geometry is evident from the fact that the metric is independent of the time coordinate t . Equivalently, the partial time derivative $\partial/\partial t$ of the Schwarzschild metric is zero. The associated Killing vector ξ^μ is then defined by

$$\xi^\mu \frac{\partial}{\partial x^\mu} = \frac{\partial}{\partial t} \quad (42)$$

so that in Schwarzschild coordinates $\{t, r, \theta, \phi\}$

$$\xi^\mu = \{1, 0, 0, 0\} . \quad (43)$$

In coordinate-independent notation, the Killing vector is

$$\boldsymbol{\xi} = \mathbf{g}_\mu \xi^\mu = \mathbf{g}_t . \quad (44)$$

This may seem like overkill – couldn't we just say that the metric is independent of time t and be done with it? The answer is that symmetries are not always evident from the metric, as will be seen in the next subsection 3.12.2.

Because the Killing vector \mathbf{g}_t is the unique timelike Killing vector of the Schwarzschild geometry, it has a definite meaning independent of the coordinate system. It follows that its scalar product with itself is a coordinate-independent scalar

$$\xi_\mu \xi^\mu = \mathbf{g}_t \cdot \mathbf{g}_t = g_{tt} = 1 - \frac{2M}{r} . \quad (45)$$

In curved spacetimes, it is hugely important to be able to identify scalars, which have a physical meaning independent of the choice of coordinates.

3.12.2 Spherical symmetry

The rotational symmetry of the Schwarzschild metric about the azimuthal axis is evident from the fact that the metric is independent of the azimuthal coordinate ϕ . The associated Killing vector is

$$\mathbf{g}_\phi \quad (46)$$

with components $\{0, 0, 0, 1\}$ in Schwarzschild coordinates $\{t, r, \theta, \phi\}$.

The Schwarzschild metric is fully spherically symmetric, not just azimuthally symmetric. Since the 3D rotation group $O(3)$ is 3-dimensional, it is to be expected that there are three

Killing vectors. You may recognize from quantum mechanics that $\partial/\partial\phi$ is (modulo factors of i and \hbar) the z -component of the angular momentum operator $\mathbf{L} = \{L_x, L_y, L_z\}$ in a coordinate system where the azimuthal axis is the z -axis. The 3 components of the angular momentum operator are given by:

$$\begin{aligned} iL_x &= y \frac{\partial}{\partial z} - z \frac{\partial}{\partial y} = -\sin\phi \frac{\partial}{\partial\theta} - \cot\theta \cos\phi \frac{\partial}{\partial\phi}, \\ iL_y &= z \frac{\partial}{\partial x} - x \frac{\partial}{\partial z} = \cos\phi \frac{\partial}{\partial\theta} - \cot\theta \sin\phi \frac{\partial}{\partial\phi}, \\ iL_z &= x \frac{\partial}{\partial y} - y \frac{\partial}{\partial x} = \frac{\partial}{\partial\phi}. \end{aligned} \quad (47)$$

The 3 rotational Killing vectors are correspondingly:

$$\begin{aligned} \text{rotation about } x\text{-axis:} & \quad -\sin\phi \mathbf{g}_\theta - \cot\theta \cos\phi \mathbf{g}_\phi, \\ \text{rotation about } y\text{-axis:} & \quad \cos\phi \mathbf{g}_\theta - \cot\theta \sin\phi \mathbf{g}_\phi, \\ \text{rotation about } z\text{-axis:} & \quad \mathbf{g}_\phi. \end{aligned} \quad (48)$$

You can check that the action of the x and y rotational Killing vectors on the metric does *not* kill the metric. For example, $iL_x g_{\phi\phi} = 2r^2 \cos\phi \sin\theta \cos\theta$ does not vanish. This example shows that a more powerful and general condition, described in the next subsection 3.12.3, is needed to establish whether a quantity is or is not a Killing vector.

Because spherical symmetry does not define a unique azimuthal axis \mathbf{g}_ϕ , its scalar product with itself $\mathbf{g}_\phi \cdot \mathbf{g}_\phi = g_{\phi\phi} = -r^2 \sin^2\theta$ is *not* a coordinate-invariant scalar. However, the sum of the scalar products of the 3 rotational Killing vectors is rotationally invariant, and is therefore a coordinate-invariant scalar

$$(-\sin\phi \mathbf{g}_\theta - \cot\theta \cos\phi \mathbf{g}_\phi)^2 + (\cos\phi \mathbf{g}_\theta - \cot\theta \sin\phi \mathbf{g}_\phi)^2 + \mathbf{g}_\phi^2 = g_{\theta\theta} + (\cot^2\theta + 1)g_{\phi\phi} = -2r^2. \quad (49)$$

This shows that the circumferential radius r is a scalar, as you would expect.

3.12.3 Killing equation

As seen in the previous subsection, a Killing vector does not always kill the metric in a given coordinate system. This is not really surprising given the arbitrariness of coordinates in GR. What is true is that a quantity is a Killing vector if and only if there exists a coordinate system such that the Killing vector kills the metric in that system.

Suppose that in some coordinate system the metric is independent of the coordinate ϕ . In problem set 2 you showed that in such a case the covariant component u_ϕ of the 4-velocity along a geodesic is constant

$$u_\phi = \text{constant}. \quad (50)$$

Equivalently

$$\xi^\nu u_\nu = \text{constant} \quad (51)$$

where ξ^ν is the associated Killing vector, whose only non-zero component is $\xi^\phi = 1$ in this particular coordinate system. The converse is also true: if $\xi^\nu u_\nu = \text{constant}$ along all geodesics, then ξ^ν is a Killing vector. The constancy of $\xi^\nu u_\nu$ along all geodesics is equivalent to the condition that its proper time derivative vanish along all geodesics

$$\frac{d\xi^\nu u_\nu}{d\tau} = 0 . \quad (52)$$

But this is equivalent to

$$0 = u^\mu D_\mu (\xi^\nu u_\nu) = u^\nu u^\mu D_\mu \xi_\nu = \frac{1}{2} u^\mu u^\nu (D_\mu \xi_\nu + D_\nu \xi_\mu) \quad (53)$$

where the second equality follows from the geodesic equation, $u^\mu D_\mu u_\nu = 0$, and the last equality is true because of the symmetry of $u^\mu u^\nu$ in $\mu \leftrightarrow \nu$. A necessary and sufficient condition for equation (53) to be true for all geodesics is that

$$\boxed{D_\mu \xi_\nu + D_\nu \xi_\mu = 0} \quad (54)$$

which is **Killing's equation**. This equation is the desired necessary and sufficient condition for ξ^ν to be a Killing vector. It is a generally covariant equation, valid in any coordinate system.

3.13 Reissner-Nordström geometry

The Reissner-Nordström geometry, discovered independently by Hans Reissner in 1916, Hermann Weyl in 1917, and Gunnar Nordström in 1918, describes the unique spherically symmetric static solution for a black hole with mass and electric charge in asymptotically flat spacetime.

3.13.1 Reissner-Nordström metric

The **Reissner-Nordström metric** for a black hole of mass M and electric charge Q is

$$\boxed{ds^2 = \left(1 - \frac{2M}{r} + \frac{Q^2}{r^2}\right) dt^2 - \left(1 - \frac{2M}{r} + \frac{Q^2}{r^2}\right)^{-1} dr^2 - r^2 d\phi^2} \quad (55)$$

which looks like the Schwarzschild metric with the replacement

$$M \rightarrow M(r) = M - \frac{Q^2}{2r} . \quad (56)$$

In fact equation (56) has a coordinate independent interpretation as the mass $M(r)$ interior to radius r , which here is the mass M at infinity, minus the mass in the electric field $E = Q/r^2$ outside r

$$\int_r^\infty \frac{E^2}{8\pi} 4\pi r^2 dr = \int_r^\infty \frac{Q^2}{8\pi r^4} 4\pi r^2 dr = \frac{Q^2}{2r} . \quad (57)$$

This seems like a Newtonian calculation of the energy in the electric field, but it turns out to be valid also in general relativity.

Real astronomical black holes probably have very little electric charge, because the Universe as a whole appears almost electrically neutral (and Maxwell's equations in fact require that the Universe in its entirety should be exactly electrically neutral), and a charged black hole would quickly neutralize itself. It would probably not neutralize itself completely, but have some small residual positive charge, because protons (positive charge) are more massive than electrons (negative charge), so it is slightly easier for a black hole to accrete protons than electrons.

Nevertheless, the Reissner-Nordström solution is of more than passing interest because its internal geometry resembles that of the Kerr solution for a rotating black hole.

3.13.2 Energy-momentum tensor

The Einstein tensor of the Reissner-Nordström metric (55) is diagonal, with elements given by

$$\begin{pmatrix} G_t^t & 0 & 0 & 0 \\ 0 & -G_r^r & 0 & 0 \\ 0 & 0 & -G_\theta^\theta & 0 \\ 0 & 0 & 0 & -G_\phi^\phi \end{pmatrix} = 4\pi \begin{pmatrix} \rho & 0 & 0 & 0 \\ 0 & p_r & 0 & 0 \\ 0 & 0 & p_\perp & 0 \\ 0 & 0 & 0 & p_\perp \end{pmatrix} = \frac{Q^2}{r^4} \begin{pmatrix} 1 & 0 & 0 & 0 \\ 0 & -1 & 0 & 0 \\ 0 & 0 & 1 & 0 \\ 0 & 0 & 0 & 1 \end{pmatrix}. \quad (58)$$

The trick of writing one index up and the other down on the Einstein tensor G_μ^ν partially cancels the distorting effect of the metric, yielding the proper energy density ρ , the proper radial pressure p_r , and transverse pressure p_\perp , up to factors of ± 1 . A more systematic way to extract proper quantities is to work in the tetrad formalism, but this will do for now.

The energy-momentum tensor is that of a radial electric field

$$E = \frac{Q}{r^2}. \quad (59)$$

Notice that the radial pressure p_r is negative, while the transverse pressure p_\perp is positive. It is no coincidence that the sum of the diagonal elements is twice the energy density, $\rho + p_r + 2p_\perp = 2\rho$.

The negative pressure, or tension, of the radial electric field produces a gravitational repulsion that dominates at small radii, and that is responsible for much of the strange phenomenology of the Reissner-Nordström geometry. The gravitational repulsion mimics the centrifugal repulsion inside a rotating black hole, for which reason the Reissner-Nordström geometry is often used a surrogate for the rotating Kerr-Newman geometry.

At this point, the statements that the energy-momentum tensor is that of a radial electric field, and that the radial tension produces a gravitational repulsion that dominates at small radii, are true but unjustified assertions.

3.13.3 Weyl tensor

As with the Schwarzschild geometry (indeed, any spherically symmetric geometry), only 1 of the 10 independent spin components of the Weyl tensor is non-vanishing, the real spin-0 component, the Weyl scalar C . The Weyl scalar for the Reissner-Nordström geometry is

$$C = -\frac{M}{r^3} + \frac{Q^2}{r^4} . \quad (60)$$

The Weyl scalar goes to infinity at zero radius

$$C \rightarrow \infty \quad \text{as } r \rightarrow 0 \quad (61)$$

signalling the presence of a real singularity at zero radius.

3.13.4 Horizons

The Reissner-Nordström geometry has not one but two horizons. The horizons occur where an object at rest in the geometry, $dr = d\theta = d\phi$, follows a null geodesic, $ds^2 = 0$, which occurs where

$$1 - \frac{2M}{r} + \frac{Q^2}{r^2} = 0 . \quad (62)$$

This is a quadratic equation in r , and it has two solutions, an **outer horizon** r_+ and an **inner horizon** r_-

$$r_{\pm} = M \pm \sqrt{M^2 - Q^2} . \quad (63)$$

It is straightforward to check that the Reissner-Nordström time coordinate t is timelike outside the outer horizon, $r > r_+$, spacelike between the horizons $r_- < r < r_+$, and again timelike inside the inner horizon $r < r_-$. Conversely, the radial coordinate r is spacelike outside the outer horizon, $r > r_+$, timelike between the horizons $r_- < r < r_+$, and spacelike inside the inner horizon $r < r_-$.

The physical meaning of this strange behavior is akin to that of the Schwarzschild geometry. As in the Schwarzschild geometry, outside the outer horizon r_+ space is falling at less than the speed of light; at the outer horizon space hits the speed of light; and inside the outer horizon space is falling faster than light. But a new ingredient appears. The gravitational repulsion caused by the negative pressure of the electric field slows down the flow of space, so that it slows back down to the speed of light at the inner horizon r_- . Inside the inner horizon space is falling at less than the speed of light.

3.13.5 Gullstrand-Painlevé metric

Deeper insight into the Reissner-Nordström geometry comes from examining its Gullstrand-Painlevé metric. The Gullstrand-Painlevé metric for the Reissner-Nordström geometry is the same as that for the Schwarzschild geometry

$$ds^2 = dt_{\text{ff}}^2 - (dr - \beta dt_{\text{ff}})^2 - r^2 d\theta^2 . \quad (64)$$

The velocity β is again the escape velocity, but this is now

$$\beta = \mp \sqrt{\frac{2M(r)}{r}} \quad (65)$$

where $M(r) = M - Q^2/2r$ is the interior mass already given as equation (56). Horizons occur where the magnitude of the velocity β equals the speed of light

$$|\beta| = 1 \quad (66)$$

which happens at the outer and inner horizons $r = r_+$ and $r = r_-$, equation (63).

The Gullstrand-Painlevé metric once again paints the picture of space falling into the black hole. Outside the outer horizon r_+ space falls at less than the speed of light, at the horizon space falls at the speed of light, and inside the horizon space falls faster than light. But the gravitational repulsion produced by the tension of the radial electric field starts to slow down the inflow of space, so that the infall velocity reaches a maximum at $r = Q^2/M$. The infall slows back down to the speed of light at the inner horizon r_- . Inside the inner horizon, the flow of space slows all the way to zero velocity, $\beta = 0$, at the turnaround radius

$$r_0 = \frac{Q^2}{2M} . \quad (67)$$

Space then turns around, the velocity β becoming positive, and accelerates back up to the speed of light. Space is now accelerating outward, to larger radii r . The outfall velocity reaches the speed of light at the inner horizon r_- , but now the motion is outward, not inward. Passing back out through the inner horizon, space is falling outward faster than light. This is not the black hole, but an altogether new piece of spacetime, a white hole. The white hole looks like a time-reversed black hole. As space falls outward, the gravitational repulsion produced by the tension of the radial electric field declines, and the outflow slows. The outflow slows back to the speed of light at the outer horizon r_+ of the white hole. Outside the outer horizon of the white hole is a new universe, where once again space is flowing at less than the speed of light.

What happens inward of the turnaround radius r_0 , equation (67)? Inside this radius the interior mass $M(r)$, equation (56), is negative, and the velocity β is imaginary. The interior mass $M(r)$ diverges to negative infinity towards the central singularity at $r \rightarrow 0$. The singularity is timelike, and infinitely gravitationally repulsive, unlike the central singularity of the Schwarzschild geometry. Is it physically realistic to have a singularity that has infinite negative mass and is infinitely gravitationally repulsive? Undoubtedly not.

3.13.6 Complete Reissner-Nordström geometry

As with the Schwarzschild geometry, it is possible to go through the steps: Reissner-Nordström coordinates \rightarrow Eddington-Finkelstein coordinates \rightarrow Kruskal-Szekeres coordinates \rightarrow Penrose coordinates. The conclusion of these constructions is that the Reissner-Nordström geometry can be analytically continued, and the complete analytic continuation

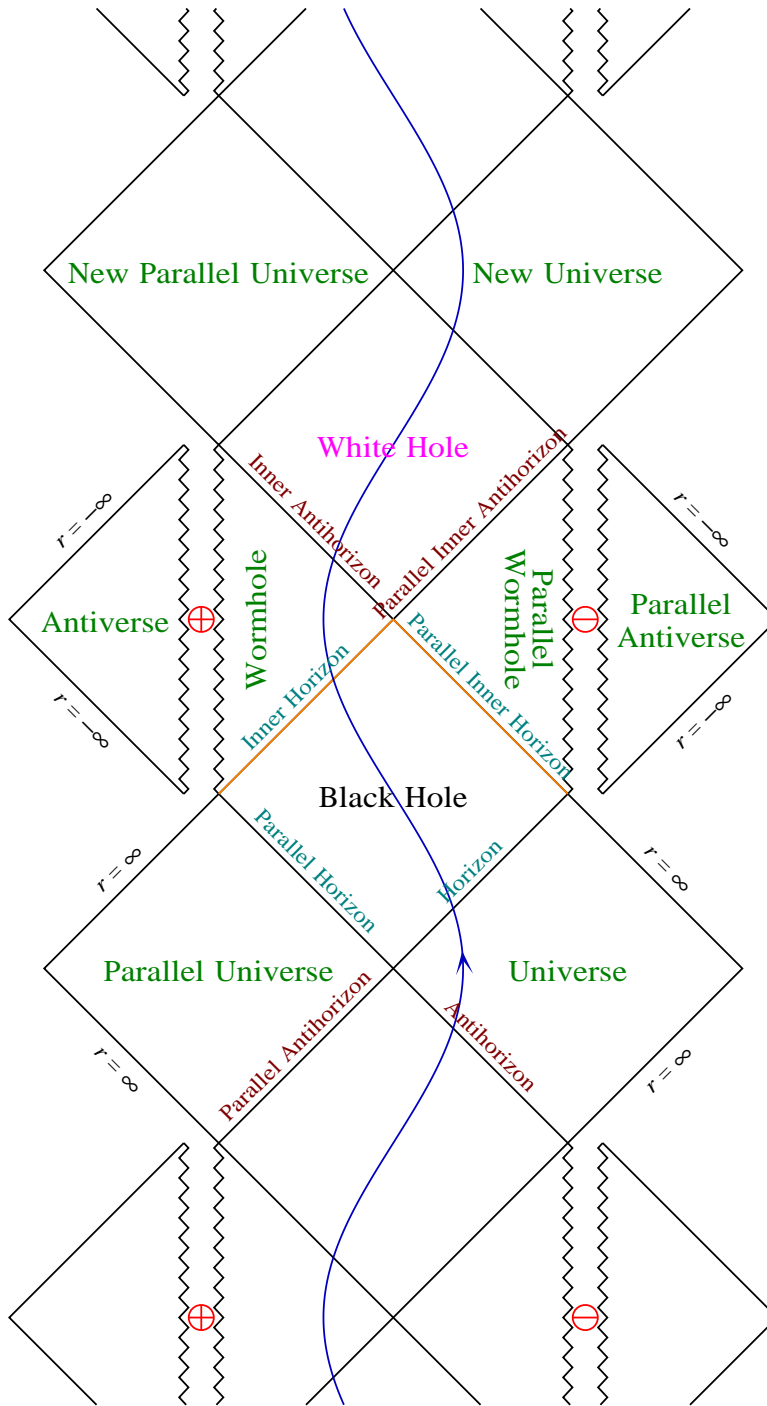


Figure 3: Penrose diagram of the complete Reissner-Nordström geometry.

consists of an infinite ladder of universes and parallel universes connected to each other by black hole \rightarrow wormhole \rightarrow white hole tunnels. I like to call the various pieces of space-time “Universe”, “Parallel Universe”, “Black Hole”, “Wormhole”, “Parallel Wormhole”, and “White Hole”. These pieces repeat in an infinite ladder.

The Wormhole and Parallel Wormhole contain separate central singularities, the “Singularity” and the “Parallel Singularity”, which are oppositely charged. If the black hole is positively charged as measured by observers in the Universe, then it is negatively charged as measured by observers in the Parallel Universe, and the Wormhole contains a positive charge singularity while the Parallel Wormhole contains a negative charge singularity.

Where does the electric charge of the Reissner-Nordström geometry “actually” reside? This comes down to the question of how observers detect the presence of charge. Observers detect charge by the electric field that it produces. Equip all (radially moving) observers with a gyroscope that they orient consistently in the same radial direction, which can be taken to be towards the black hole as measured by observers in the Universe. Observers in the Parallel Universe find that their gyroscope is pointed away from the black hole. Inside the black hole, observers from either Universe agree that the gyroscope is pointed towards the Wormhole, and away from the Parallel Wormhole. All observers agree that the electric field is pointed in the same radial direction. Observers who end up inside the Wormhole measure an electric field that appears to emanate from the Singularity, and which they therefore attribute to charge in the Singularity. Observers who end up inside the Parallel Wormhole measure an electric field that appears to emanate in the opposite direction from the Parallel Singularity, and which they therefore attribute to charge of opposite sign in the Parallel Singularity. Strange, but all consistent.

3.13.7 Antiverse: Reissner-Nordström geometry with negative mass

It is also possible to consider the Reissner-Nordström geometry for negative values of the radius r . I call the extension to negative r the “Antiverse”. There is also a “Parallel Antiverse”.

Changing the sign of r in the Reissner-Nordström metric (55) is equivalent to changing the sign of the mass M . Thus the Reissner-Nordström metric with negative r describes a charged black hole of negative mass

$$M < 0 . \tag{68}$$

The negative mass black hole is gravitationally repulsive at all radii, and it has no horizons.

3.13.8 Ingoing, outgoing

The Black Hole in the Reissner-Nordström geometry is bounded at its inner edge by not one but two inner horizons. The two distinct horizons play a crucial role in the mass inflation instability described in §3.13.9 below.

The inner horizons can be called ingoing and outgoing. Persons freely falling in the Black Hole region are all moving inward in coordinate radius r , but they may be moving either

forward or backward in Reissner-Nordström coordinate time t . The conserved energy along a geodesic is positive if the time coordinate t is increasing, negative if the time coordinate t is decreasing. Persons with positive energy are **ingoing**, while persons with negative energy are **outgoing**. Both ingoing and outgoing persons fall inward, to smaller radii, but ingoing persons think that the inward direction is towards the Wormhole, while outgoing persons think that the inward direction is in the opposite direction, towards the Parallel Wormhole. Ingoing persons fall through the ingoing inner horizon, while outgoing persons fall through the outgoing inner horizon.

Geodesics in the Universe and Wormhole regions necessarily have positive energy, because coordinate time t is moving forwards in these regions. Conversely, geodesics in the Parallel Universe and Parallel Wormhole regions necessarily have negative energy, because coordinate time t is moving backwards in these regions. Of course, all observers, wherever they may be, always perceive their own proper time to be moving forward in the usual fashion, at the rate of one second per second.

3.13.9 Mass inflation instability

Roger Penrose (1968) first pointed out that a person passing through the outgoing inner horizon (also called the Cauchy horizon) of the Reissner-Nordström geometry would see the outside Universe infinitely blueshifted, and he suggested that this would destabilize the geometry. Perturbation theory calculations, starting with Simpson & Penrose (1973) and culminating with Chandrasekhar and Hartle (1982), confirmed that waves become infinitely blueshifted as they approach the outgoing inner horizon, and that their energy density diverges. The perturbation theory calculations were widely construed as indicating that the Reissner-Nordström geometry was “unstable”, although the precise nature of this instability remained obscure.

It was not until a seminal paper by Poisson & Israel (1990) that the true nonlinear nature of the instability at the inner horizon was clarified. Poisson & Israel showed that the Reissner-Nordström geometry is subject to an exponentially growing instability which they dubbed **mass inflation**. The term refers to the fact that the interior mass $M(r)$ grows exponentially during mass inflation. The interior mass $M(r)$ has the property of being a gauge-invariant, scalar quantity, so it has a physical meaning independent of the coordinate system.

What causes mass inflation? Actually it has nothing to do with mass: the inflating mass is just a symptom of the underlying cause. What causes mass inflation is relativistic counter-streaming between ingoing and outgoing streams. As the Penrose diagram of the Reissner-Nordström geometry shows, ingoing and outgoing streams must drop through separate ingoing and outgoing inner horizons into separate pieces of spacetime, the Wormhole and the Parallel Wormhole. The regions of spacetime must be separate because coordinate time t is timelike in both regions, but going in opposite directions in the two regions, forward in the Wormhole, backward in the Parallel Wormhole. In other words, ingoing and outgoing streams cannot co-exist in the same subluminal region of spacetime because they would have to be moving in opposite directions in time, which cannot be.

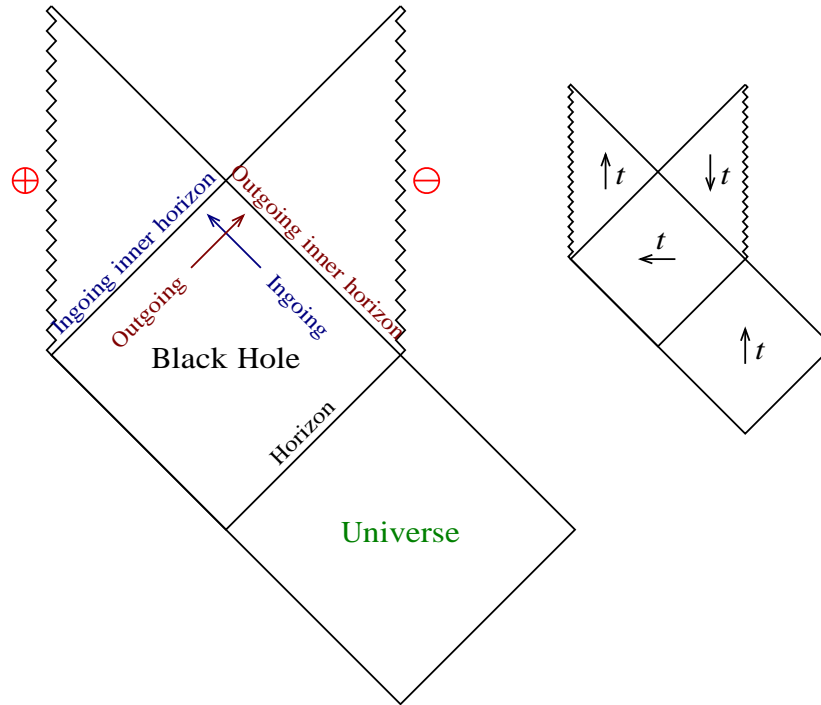


Figure 4: Penrose diagram illustrating why the Reissner-Nordström geometry is subject to the mass inflation instability. Ingoing and outgoing streams just outside the inner horizon must pass through separate ingoing and outgoing inner horizons into causally separated pieces of spacetime where the timelike time coordinate t goes in opposite directions. To accomplish this, the ingoing and outgoing streams must exceed the speed of light through each other, which physically they cannot do. The mass inflation instability is driven by the pressure of the relativistic counter-streaming between ingoing and outgoing streams. The inset shows the direction of coordinate time t in the various regions. Proper time of course always increases upward in a Penrose diagram.

In the Reissner-Nordström geometry, ingoing and outgoing streams resolve their differences by exceeding the speed of light relative to each other, and passing into causally separated regions. As the ingoing and outgoing streams drop through their respective inner horizons, they each see the other stream infinitely blueshifted.

In reality however, this cannot occur: ingoing and outgoing streams cannot exceed the speed of light relative to each other. Instead, as the ingoing and outgoing streams move ever faster through each other in their effort to drop through the inner the horizon, their counter-streaming generates a radial pressure. The pressure, which is positive, exerts an inward gravitational force. As the counter-streaming approaches the speed of light, the gravitational force produced by the counter-streaming pressure eventually exceeds the gravitational force produced by the background Reissner-Nordström geometry. At this point, mass inflation begins.

The gravitational force produced by the counter-streaming is inwards, but, in the strange way that general relativity operates, the inward direction is in opposite directions for the ingoing streams, towards the black hole for the ingoing stream, and away from the black hole for the outgoing stream. Consequently the counter-streaming pressure simply accelerates the ingoing and outgoing streams ever faster through each other. The result is an exponential feedback instability. The increasing pressure accelerates the streams faster through each other, which increases the pressure, which increases the acceleration.

The interior mass is not the only thing that increases exponentially during mass inflation. The proper density and pressure, and the Weyl scalar (all gauge-invariant scalars) exponentiate together.

3.13.10 Inevitability of mass inflation

Mass inflation requires the simultaneous presence of both ingoing and outgoing streams near the inner horizon. Will that happen in real black holes? Any real black hole will of course accrete matter from its surroundings, so certainly there will be a stream of one kind or another (ingoing or outgoing) inside the black hole. But is it guaranteed that there will also be a stream of the other kind? The answer is probably.

One of the remarkable features of the mass inflation instability is that, as long as ingoing and outgoing streams are both present, the smaller the perturbation the more violent the instability. That is, if say the outgoing stream is reduced to a tiny trickle compared to the ingoing stream (or vice versa), then the length scale (and time scale) over which mass inflation occurs gets shorter. During mass inflation, as the counter-streaming streams drop through an interval Δr of circumferential radius, the interior mass $M(r)$ increases exponentially with length scale l

$$M(r) \propto e^{\Delta r/l} . \quad (69)$$

It turns out that the inflationary length scale l is proportional to the accretion rate

$$l \propto \dot{M} \quad (70)$$

so that smaller accretion rates produce more violent inflation. Physically, the smaller accretion rate, the closer the streams must approach the inner horizon before the pressure of their counter-streaming begins to dominate the gravitational force. The distance between the inner horizon and where mass inflation begins effectively sets the length scale l of inflation.

Given this feature of mass inflation, that the tinier the perturbation the more rapid the growth, it seems almost inevitable that mass inflation must occur inside real black holes. Even the tiniest piece of stuff going the wrong way is apparently enough to trigger the mass inflation instability.

One way to avoid mass inflation inside a real black hole is to have a large level of dissipation inside the black hole, sufficient to reduce the charge (or spin) to zero near the singularity. In that case the central singularity reverts to being spacelike, like the Schwarzschild singularity. While the electrical conductivity of a realistic plasma is more than adequate to neutralize

a charged black hole, angular momentum transport is intrinsically a much weaker process, and it is not clear whether the dissipation of angular momentum might be large enough to eliminate the spin near the singularity of a rotating black hole. There has been no research on the latter subject.

3.13.11 The black hole particle accelerator

A good way to think conceptually about mass inflation is that it acts like a particle accelerator. The counter-streaming pressure accelerates ingoing and outgoing streams through each other at an exponential rate, so that a Lagrangian gas element spends equal amounts of proper time accelerating through equal decades of counter-streaming velocity. The center of mass energy easily exceeds the Planck energy, where quantum mechanics presumably comes into play.

Mass inflation is expected to occur just above the inner horizon of a black hole. In a realistic rotating astronomical black hole, the inner horizon is likely to be at a considerable fraction of the radius of the outer horizon. Thus the black hole accelerator operates not near a central singularity, but rather at a macroscopically huge scale. This machine is truly monstrous.

Undoubtedly much fascinating physics occurs in the black hole particle accelerator. The situation is far more extreme than anywhere else in our Universe today. Who knows what Nature does there? To my knowledge, there has been no research on the subject.

3.13.12 The X point

The point in the Reissner-Nordström geometry where the ingoing and outgoing inner horizons intersect, the X point, is a special one. This is the point through which geodesics of zero energy must pass. Persons with zero energy who reach the X point see both ingoing and outgoing streams, coming from opposite directions, infinitely blueshifted.

3.13.13 Extremal Reissner-Nordström geometry

So far the discussion of the Reissner-Nordström geometry has centered on the case $Q < M$ (or more generally, $|Q| < |M|$) where there are separate outer and inner horizons. In the special case that the charge and mass are equal,

$$Q = M , \tag{71}$$

the inner and outer horizons merge into one, $r_+ = r_-$, equation (63). This special case describes the **extremal Reissner-Nordström geometry**.

The extremal Reissner-Nordström geometry proves to be of particular interest in quantum gravity because its Hawking temperature is zero, and in string theory because extremal black holes arise as solutions under certain duality transformations.

The Penrose diagram of the extremal Reissner-Nordström geometry is different from that of the standard Reissner-Nordström geometry.

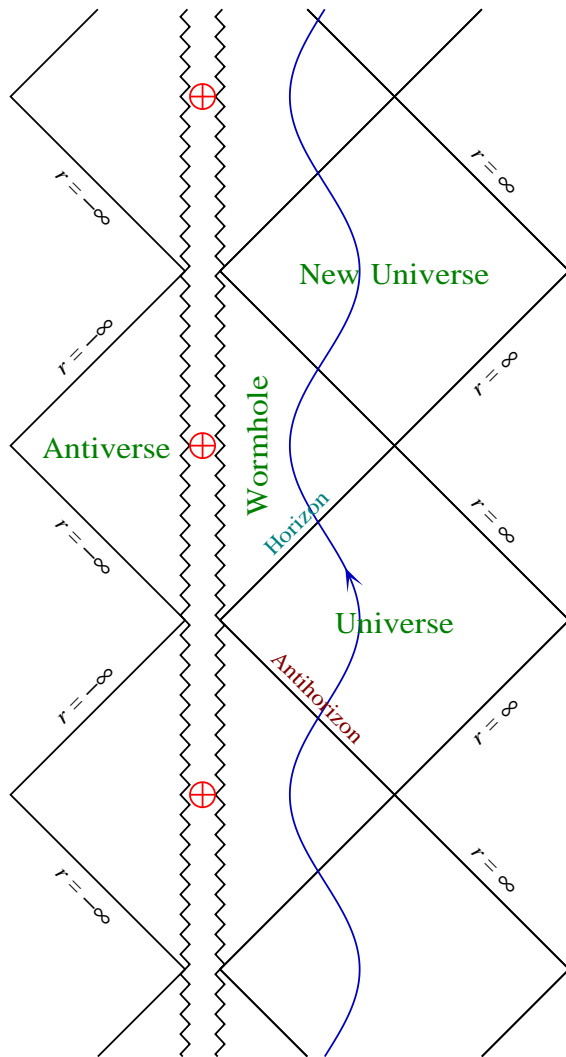


Figure 5: Penrose diagram of the extremal Reissner-Nordström geometry.

3.13.14 Reissner-Nordström geometry with charge exceeding mass

The Reissner-Nordström geometry with charge greater than mass,

$$Q > M , \tag{72}$$

has no horizons. The change in geometry from an extremal black hole, with horizon at finite radius $r_+ = r_- = M$, to one without horizons is discontinuous. This suggests that there is no way to pack a black hole with more charge than its mass. Indeed, if you try to force additional charge into an extremal black hole, then the work needed to do so increases its mass so that the charge Q does not exceed its mass M .

Real fundamental particles nevertheless have charge far exceeding their mass. For example, the charge-to-mass ratio of a proton is

$$\frac{e}{m_p} \approx 10^{18} \tag{73}$$

where e is the square root of the fine-structure constant $\alpha \equiv e^2/\hbar c \approx 1/137$, and $m_p \approx 10^{-19}$ is the mass of the proton in Planck units. However, the Schwarzschild radius of such a fundamental particle is far tinier than its Compton wavelength $\sim \hbar/m$ (or its classical radius $e^2/m = \alpha\hbar/m$), so quantum mechanics, not general relativity, governs the structure of these fundamental particles.

3.13.15 Reissner-Nordström geometry with imaginary charge

It is possible formally to consider the Reissner-Nordström geometry with imaginary charge Q

$$Q^2 < 0 . \tag{74}$$

This is completely unphysical. If charge were imaginary, then electromagnetic energy would be negative.

However, the Reissner-Nordström metric with $Q^2 < 0$ is well-defined, and it is possible to calculate geodesics in that geometry. What makes the geometry interesting is that the singularity, instead of being gravitationally repulsive, becomes gravitationally attractive. Thus particles, instead of bouncing off the singularity, are attracted to it, and it turns out to be possible to continue geodesics through the singularity. Mathematically, the geometry can be considered as the Kerr-Newman geometry in the limit of zero spin. In the Kerr-Newman geometry, geodesics can pass from positive to negative radius r , and the passage through the singularity of the Reissner-Nordström geometry can be regarded as this process in the limit of zero spin.

Suffice to say that it is intriguing to see what it looks like to pass through the singularity of a charged black hole of imaginary charge, however unrealistic. The Penrose diagram is even more eventful than that for the usual Reissner-Nordström geometry.

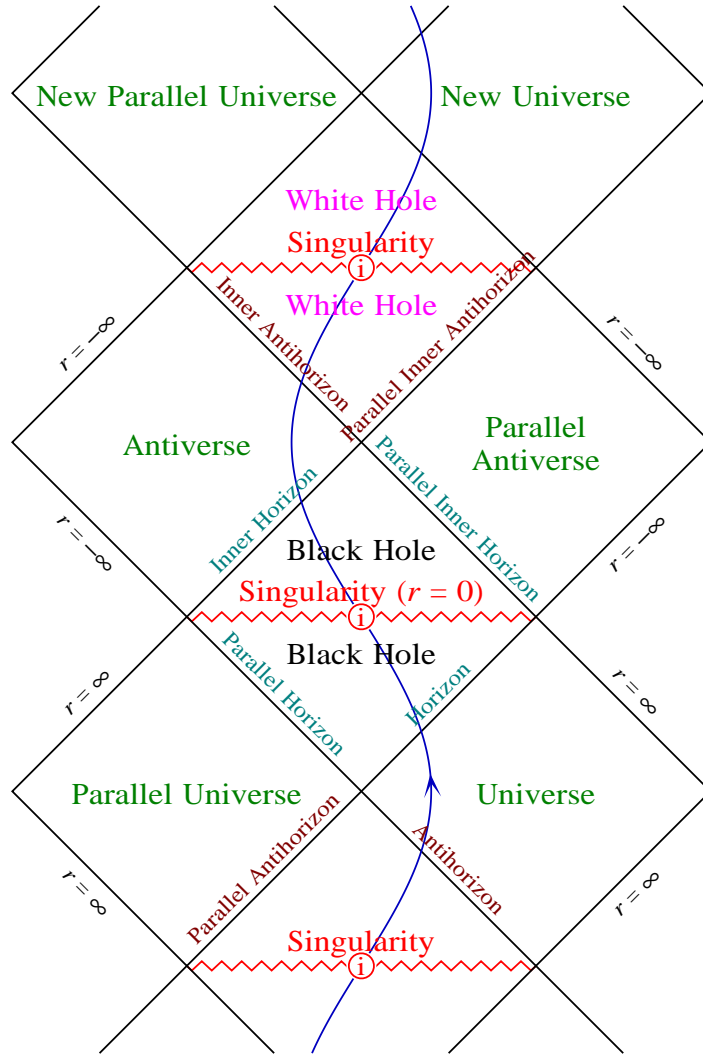


Figure 6: Penrose diagram of the Reissner-Nordström geometry with imaginary charge Q . If charge were imaginary, then electromagnetic energy would be negative, which is completely unphysical. But the metric is well-defined, and the spacetime is fun.

3.14 Kerr-Newman geometry

The geometry of a stationary, rotating, uncharged black hole in asymptotically flat empty space was discovered unexpectedly by Roy Kerr in 1963. Kerr's (2007) own account of the history of the discovery is at <http://arxiv.org/abs/0706.1109>. You can read in that paper that the discovery was not mere chance: Kerr used sophisticated mathematical methods to make it. The extension to a rotating charged black hole was made shortly thereafter by Newman et al. in 1965.

The importance of the Kerr-Newman geometry stems in part from the no-hair theorem, which states that this geometry is the unique end state of spacetime outside the horizon of an undisturbed black hole in asymptotically flat space.

3.14.1 Boyer-Lindquist metric

The Boyer-Lindquist metric of the Kerr-Newman geometry is

$$ds^2 = \frac{\Delta}{\rho^2} (dt - a \sin^2\theta d\phi)^2 - \frac{\rho^2}{\Delta} dr^2 - \rho^2 d\theta^2 - \frac{R^4 \sin^2\theta}{\rho^2} \left(d\phi - \frac{a}{R^2} dt \right)^2 \quad (75)$$

where R and ρ are defined by

$$R \equiv \sqrt{r^2 + a^2}, \quad \rho \equiv \sqrt{r^2 + a^2 \cos^2\theta}, \quad (76)$$

and Δ is the horizon function defined by

$$\Delta \equiv R^2 - 2Mr + Q^2. \quad (77)$$

At large radius r , the Boyer-Lindquist metric is

$$ds^2 \rightarrow \left(1 - \frac{2M}{r}\right) dt^2 - \left(1 + \frac{2M}{r}\right) dr^2 - r^2 (d\theta^2 + \sin^2\theta d\phi^2) + \frac{4aM \sin^2\theta}{r} dt d\phi. \quad (78)$$

Comparison of this metric to the metric of a weak field establishes that M is the mass of the black hole and a is its angular momentum per unit mass. For positive a , the black hole rotates right-handedly about its polar axis $\theta = 0$.

3.14.2 Oblate spheroidal coordinates

Boyer-Lindquist coordinates r, θ, ϕ are **oblate spheroidal** coordinates (not polar coordinates). Corresponding Cartesian coordinates are

$$\begin{aligned} x &= R \sin\theta \cos\phi, \\ y &= R \sin\theta \sin\phi, \\ z &= r \cos\theta. \end{aligned} \quad (79)$$

Surfaces of constant r are confocal oblate spheroids, satisfying

$$\frac{x^2 + y^2}{r^2 + a^2} + \frac{z^2}{r^2} = 1 . \quad (80)$$

Equation (80) implies that the spheroidal coordinate r is given in terms of x, y, z by the quadratic equation

$$r^4 - r^2(x^2 + y^2 + z^2 - a^2) - a^2 z^2 = 0 . \quad (81)$$

3.14.3 Time and rotation symmetries

The Boyer-Linquist metric coefficients are independent of the time coordinate t and of the azimuthal angle ϕ . This shows that the Kerr-Newman geometry has time translation symmetry, and rotational symmetry about its azimuthal axis. The time and rotation symmetries means that the tangent vectors \mathbf{g}_t and \mathbf{g}_ϕ in Boyer-Linquist coordinates are Killing vectors. It follows that their scalar products

$$\begin{aligned} \mathbf{g}_t \cdot \mathbf{g}_t &= g_{tt} = \frac{1}{\rho^2} (\Delta - a^2 \sin^2 \theta) , \\ \mathbf{g}_t \cdot \mathbf{g}_\phi &= g_{t\phi} = \frac{a \sin^2 \theta}{\rho^2} (R^2 - \Delta) , \\ \mathbf{g}_\phi \cdot \mathbf{g}_\phi &= g_{\phi\phi} = -\frac{\sin^2 \theta}{\rho^2} (R^4 - a^2 \sin^2 \theta \Delta) , \end{aligned} \quad (82)$$

are all gauge-invariant scalar quantities. As will be seen below, $g_{tt} = 0$ defines the boundary of ergospheres, $g_{t\phi} = 0$ defines the turnaround radius, and $g_{\phi\phi} = 0$ defines the boundary of the toroidal region containing closed timelike curves.

The Boyer-Linquist time t and azimuthal angle ϕ are arranged further to satisfy the condition that \mathbf{g}_t and \mathbf{g}_ϕ are each orthogonal to both \mathbf{g}_r and \mathbf{g}_θ .

3.14.4 Ring singularity

The Kerr-Newman geometry contains a **ring singularity** where the Weyl tensor (102) diverges, at

$$\boxed{r = 0 \text{ and } \theta = \pi/2} . \quad (83)$$

The ring singularity is at the focus of the confocal ellipsoids of the Boyer-Linquist metric. Physically, the singularity is kept open by the centrifugal force.

3.14.5 Horizons

The horizon of a Kerr-Newmman black hole rotates, as observed by a distant observer, so it is incorrect to try to solve for the location of the horizon by assuming that it is at rest. The worldline of a photon that sits on the horizon, battling against the inflow of space, remains

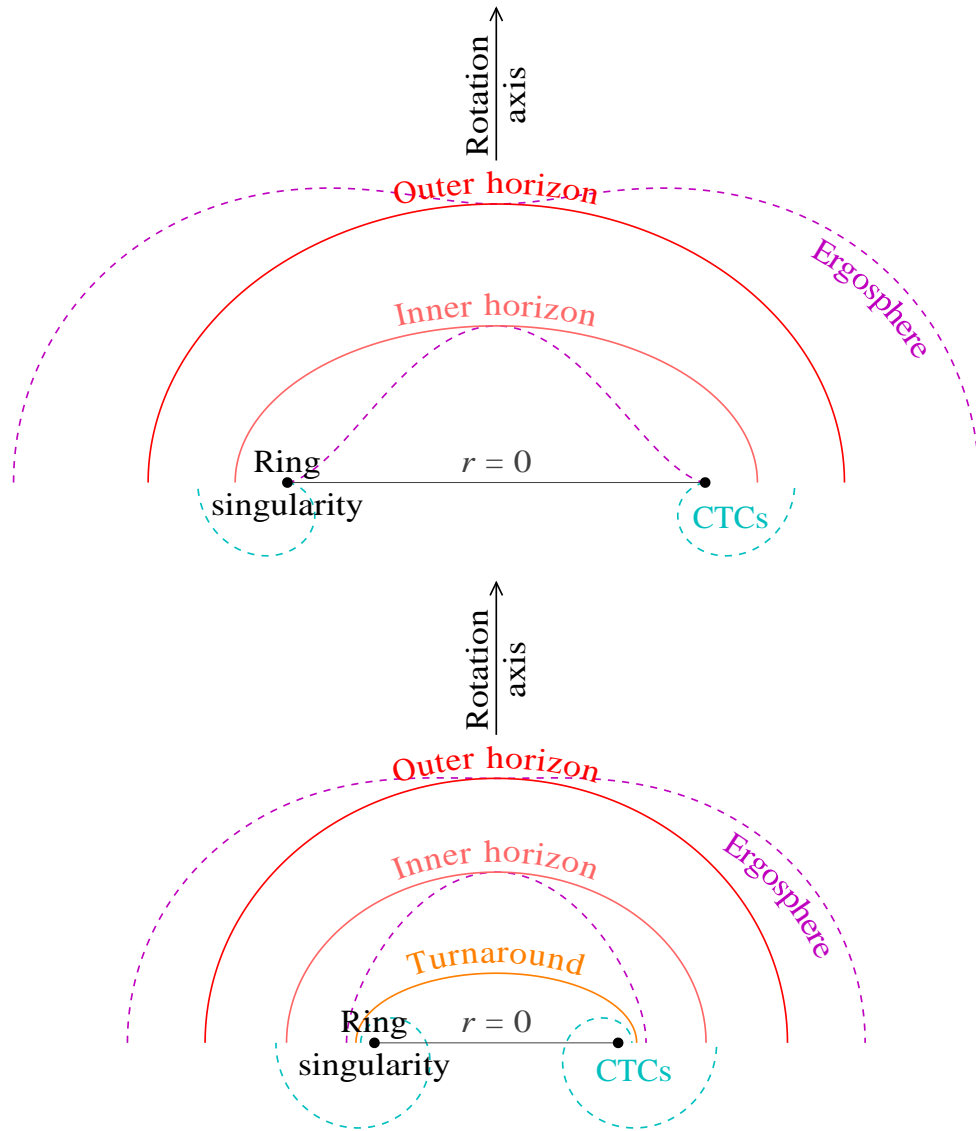


Figure 7: Geometry of (upper) a Kerr black hole with spin parameter $a = 0.96$, and (lower) a Kerr-Newman black hole with charge $Q = 0.8$ and spin parameter $a = 0.56$. The upper half of each diagram shows $r \geq 0$, while the lower half shows $r \leq 0$, the Antiverse. The outer and inner horizons are confocal oblate spheroids whose focus is the ring singularity. For the Kerr geometry, the turnaround radius is at $r = 0$. CTCs are closed timelike curves.

at fixed radius r and polar angle θ , but it moves in time t and azimuthal angle ϕ . The photon's 4-velocity is $v^\mu = \{v^t, 0, 0, v^\phi\}$, and the condition that it is on a null geodesic is

$$0 = v_\mu v^\mu = g_{\mu\nu} v^\mu v^\nu = g_{tt}(v^t)^2 + 2g_{t\phi} v^t v^\phi + g_{\phi\phi}(v^\phi)^2. \quad (84)$$

This equation has solutions provided that the determinant of the 2×2 matrix of metric coefficients in t and ϕ is less than or equal to zero (why?). The determinant is

$$g_{tt}g_{\phi\phi} - g_{t\phi}^2 = -\sin^2\theta \Delta \quad (85)$$

where Δ is the horizon function defined above, equation (77). Thus if $\Delta \geq 0$, then there exist null geodesics such that a photon can be instantaneously at rest in r and θ , whereas if $\Delta < 0$, then no such geodesics exist. The boundary

$$\Delta = 0 \quad (86)$$

defines the location of horizons. With Δ given by equation (77), equation (86) gives **outer** and **inner horizons** at

$$\boxed{r_\pm = M \pm \sqrt{M^2 - Q^2 - a^2}}. \quad (87)$$

Between the horizons Δ is negative, and photons cannot be at rest. This is consistent with the picture that space is falling faster than light between the horizons.

3.14.6 Angular velocity of the horizon

The Boyer-Linquist metric (78) has been cunningly written so that you can read off the angular velocity of the horizon as observed by observers at rest at infinity. The horizon is at $dr = d\theta = 0$ and $\Delta = 0$, and then the null condition $ds^2 = 0$ implies that the angular velocity is

$$\frac{d\phi}{dt} = \frac{a}{R^2}. \quad (88)$$

The derivative is with respect to the proper time t of observers at rest at infinity, so this is the angular velocity observed by such observers.

3.14.7 Ergospheres

There are finite regions, just outside the outer horizon and just inside the inner horizon, within which the worldline of an object at rest, $dr = d\theta = d\phi = 0$, is spacelike. These regions, called **ergospheres**, are places where nothing can remain at rest (the place where little children come from). Objects can escape from within the outer ergosphere (whereas they cannot escape from within the outer horizon), but they cannot remain at rest there. A distant observer will see any object within the outer ergosphere being dragged around by the rotation of the black hole. The direction of dragging is the same as the rotation direction of the black hole in both outer and inner ergospheres.

The boundary of the ergosphere is at

$$g_{tt} = 0 \quad (89)$$

which occurs where

$$\Delta = a^2 \sin^2 \theta . \quad (90)$$

Equation (90) has two solutions, the outer and inner ergospheres. The outer and inner ergospheres touch respectively the outer and inner horizons at the poles, $\theta = 0$ and π .

3.14.8 Antiverse

The surface at zero radius, $r = 0$, forms a disk bounded by the ring singularity. Objects can pass through this disk into the region at negative radius, $r < 0$, the **Antiverse**.

Changing the sign of r in the Boyer-Lindquist metric (78) is equivalent to changing the sign of the mass M . Thus the Boyer-Lindquist metric with negative r describes a rotating black hole of negative mass

$$M < 0 . \quad (91)$$

3.14.9 Closed timelike curves

Inside the inner horizon there is a toroidal region around the ring singularity within which the light cone in t - ϕ coordinates opens up to the point that ϕ as well as t are timelike coordinates. The direction of increasing proper time along t is t increasing, and along ϕ is ϕ decreasing, which is retrograde. Within the toroidal region, there exist timelike trajectories that go either forwards or backwards in coordinate time t as they wind retrograde around the toroidal tunnel. Because the ϕ coordinate is periodic, these timelike curves connect not only the past to the future (the usual case), but also the future to the past, which violates causality. In particular, as first pointed out by Carter (1968), there exist **closed timelike curves** (CTCs), trajectories that connect to themselves, connecting their own future to their own past, and repeating interminably, like Sisyphus pushing his rock up the mountain.

The boundary of this toroidal region is at

$$g_{\phi\phi} = 0 \quad (92)$$

which occurs where

$$\frac{R^4}{\Delta} = a^2 \sin^2 \theta . \quad (93)$$

In the uncharged Kerr geometry the CTC torus is entirely at negative radius, $r < 0$, but in the Kerr-Newman geometry the CTC torus extends to positive radius.

3.14.10 Carter's fourth integral of motion

Geodesics in the Kerr-Newman geometry have the usual constants of motion associated with conservation of energy, conservation of angular momentum about the axis, and conservation of rest mass. For a massive particle, the 4-velocity $u^\nu \equiv dx^\nu/d\tau$ satisfies

$$u_t = E , \quad u_\phi = -L_z , \quad u_\nu u^\nu = 1 \quad (94)$$

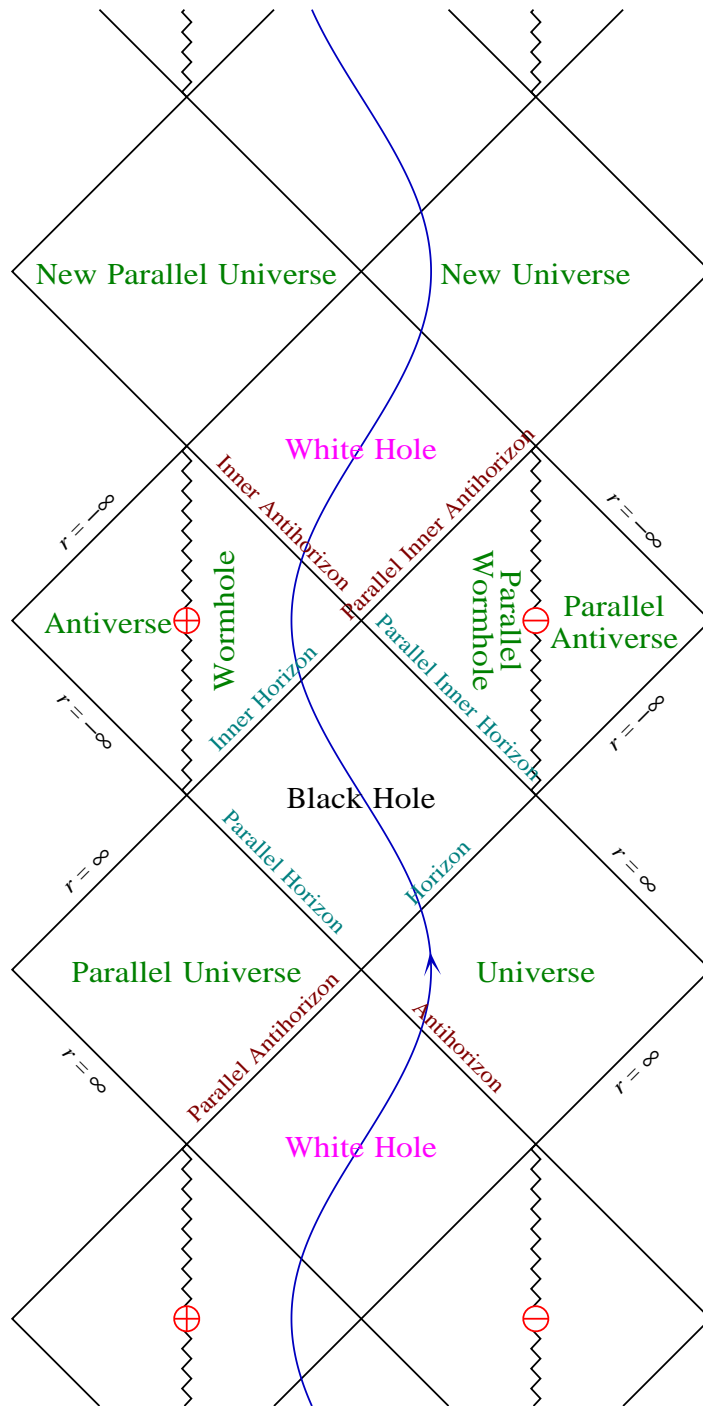


Figure 8: Penrose diagram of the Kerr-Newman geometry. The diagram is similar to that of the Reissner-Nordström geometry, except that it is possible to pass through the disk at $r = 0$ from the Wormhole region into the Antiverse region. This Penrose diagram, which represents a slice at fixed θ and ϕ , does not capture the full richness of the geometry, which contains closed timelike curves in a torus around the ring singularity.

where E is the mass per unit rest mass, and L_z is the angular momentum per unit rest mass. The case of massless particles follows from equations (94) by taking the limit of infinite energy per unit rest mass, $E \rightarrow \infty$, and introducing an affine parameter defined by $\lambda \equiv \tau/E$. For massless particles, the 4-velocity $v^\nu \equiv dx^\nu/d\lambda$ then satisfies

$$v_t = 1, \quad v_\phi = -J_z, \quad v_\nu v^\nu = 0. \quad (95)$$

Carter (1968) was able to show by separation of variables in the Hamilton-Jacobi equations that a fourth integral of motion exists

$$\mathcal{Q} = u_\theta^2 + \cos^2\theta \left[\frac{L_z^2}{\sin^2\theta} - a^2(E^2 - 1) \right] \quad (96)$$

for massive particles, or

$$\mathcal{Q} = v_\theta^2 + \cos^2\theta \left[\frac{J_z^2}{\sin^2\theta} - a^2 \right] \quad (97)$$

for massless particles. The four integrals of motion provide a complete solution for geodesics in the Kerr-Newman geometry.

3.14.11 Principal null congruences

A null congruence is a space-filling, non-overlapping set of null geodesics. In the Kerr-Newman geometry there is a special set of null geodesics, the ingoing and outgoing **principal null congruences**, with respect to which the symmetries of the geometry are especially apparent. Photons that hold steady on the horizon are members of the outgoing principal null congruence. The energy-momentum tensor is diagonal in a locally inertial frame aligned with the ingoing or outgoing principal null congruence. The Weyl tensor, decomposed into spin components in the locally inertial frame of the principal null congruences, contains only spin-0 components.

The Boyer-Linquist metric (78) has been carefully written so that the behavior of the principal null congruences is manifest. Along the principal null congruences, the final two terms of the Boyer-Linquist line element (78) vanish

$$d\theta = d\phi - \frac{a}{R^2} dt = 0. \quad (98)$$

Solving the null condition $ds^2 = 0$ on the rest of the metric yields the photon 4-velocity $v^\mu \equiv dx^\mu/d\lambda$ on the principal null congruences

$$v^t = \frac{R^2}{\Delta}, \quad v^r = \pm 1, \quad v^\theta = 0, \quad v^\phi = \frac{a}{\Delta}. \quad (99)$$

In the regions outside the outer horizon or inside the inner horizon, the \pm sign in front of v^r is + for outgoing, - for ingoing geodesics. Between the outer and inner horizons, v^r is negative in the Black Hole region, and positive in the White Hole region, while v^t and v^ϕ are positive for ingoing, negative for outgoing geodesics. The angular momentum per unit

energy J_z of photons along the principal null congruences is not zero (perhaps surprisingly), but is

$$J_z = a \sin^2 \theta \quad (100)$$

with the same sign for both ingoing and outgoing geodesics.

3.14.12 Energy-momentum tensor

The Einstein tensor of the Kerr-Newman geometry in Boyer-Linquist coordinates is a bit of a mess, so I won't write it down. When we have done tetrads we will find that, in a locally inertial frame aligned with the ingoing or outgoing principal null congruences, the Einstein tensor is diagonal, and that the proper density ρ , the proper radial pressure p_r , and the proper transverse pressure p_\perp in that frame are (do not confuse the notation ρ for proper density with the radial parameter ρ , equation (76), of the Boyer-Linquist metric)

$$\rho = -p_r = p_\perp = \frac{Q^2}{4\pi\rho^4} . \quad (101)$$

This looks like the energy-momentum tensor (58) of the Reissner-Nordström geometry with the replacement $r \rightarrow \rho$. The energy-momentum is that of an electric field produced by a charge Q seemingly located at the singularity.

3.14.13 Weyl tensor

The 10 components of the Weyl tensor can be decomposed as usual into 5 complex components of spin 0, ± 1 , and ± 2 . In a locally inertial frame aligned with the ingoing or outgoing principal null congruences, the only non-vanishing component is the spin-0 component, the Weyl scalar C , but in contrast to the Schwarzschild and Reissner-Nordström geometries the spin-0 component is complex, not real:

$$C = -\frac{1}{(r - ia \cos \theta)^3} \left(M - \frac{Q^2}{r + ia \cos \theta} \right) . \quad (102)$$

3.14.14 Doran coordinates

For the Kerr-Newman geometry, the analog of the Gullstrand-Painlevé metric is the Doran (2000) metric

$$\boxed{ds^2 = dt_{\text{ff}}^2 - \left[\frac{\rho}{R} dr - \beta \frac{R}{\rho} (dt_{\text{ff}} - a \sin^2 \theta d\phi_{\text{ff}}) \right]^2 - \rho^2 d\theta^2 - R^2 \sin^2 \theta d\phi_{\text{ff}}^2} \quad (103)$$

where the free-fall time t_{ff} and azimuthal angle ϕ_{ff} are related to the Boyer-Linquist time t and azimuthal angle ϕ by

$$dt_{\text{ff}} = dt - \frac{\beta}{1 - \beta^2} dr , \quad d\phi_{\text{ff}} = \phi - \frac{a\beta}{R^2(1 - \beta^2)} dr . \quad (104)$$

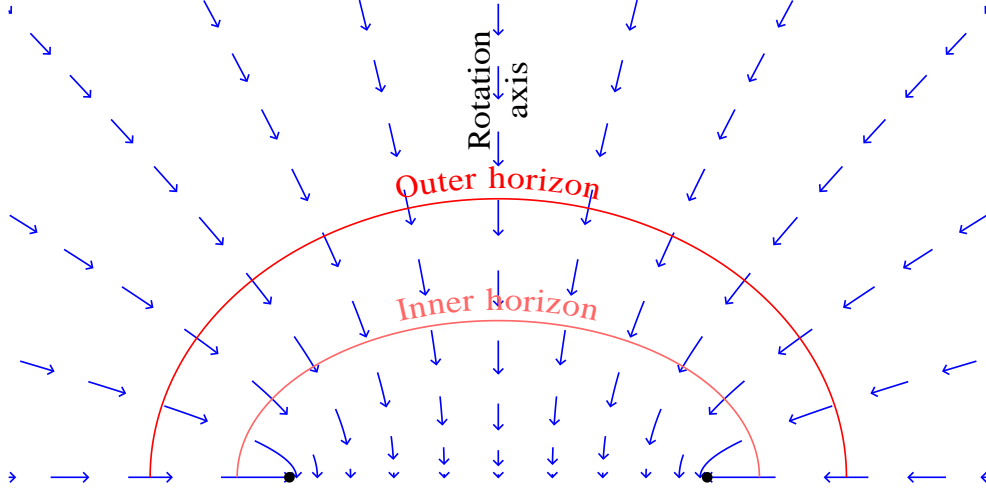


Figure 9: Geometry of a Kerr black hole with spin parameter $a = 0.96$. The arrows show the velocity β in the Doran metric. The flow follows lines of constant θ , which form nested hyperboloids orthogonal to and confocal with the nested spheroids of constant r .

The free-fall time t_{ff} is the proper time experienced by persons who free-fall from rest at infinity, with zero angular momentum. They follow trajectories of fixed θ and ϕ_{ff} , with radial velocity $dr/dt_{\text{ff}} = \beta$. In other words, the 4-velocity $u^\nu \equiv dx^\nu/d\tau$ of such free-falling observers is

$$u^{t_{\text{ff}}} = 1, \quad u^r = \beta, \quad u^\theta = 0, \quad u^{\phi_{\text{ff}}} = 0. \quad (105)$$

For the Kerr-Newman geometry, the velocity β is

$$\beta = \mp \frac{\sqrt{2Mr - Q^2}}{R} \quad (106)$$

where the \mp sign is $-$ (infalling) for black hole solutions, and $+$ (outfalling) for white hole solutions.

Horizons occur where the magnitude of the velocity β equals the speed of light

$$\beta = \mp 1. \quad (107)$$

The boundaries of ergospheres occur where the velocity is

$$\beta = \mp \frac{\rho}{R}. \quad (108)$$

The turnaround radius is where the velocity is zero

$$\beta = 0. \quad (109)$$

The region containing closed timelike curves is bounded by the imaginary velocity

$$\beta = i \frac{\rho}{a \sin \theta}. \quad (110)$$

3.15 Extremal Kerr-Newman geometry

The Kerr-Newman geometry is called extremal when the outer and inner horizons coincide, $r_+ = r_-$, which occurs where

$$M^2 = Q^2 + a^2 . \quad (111)$$

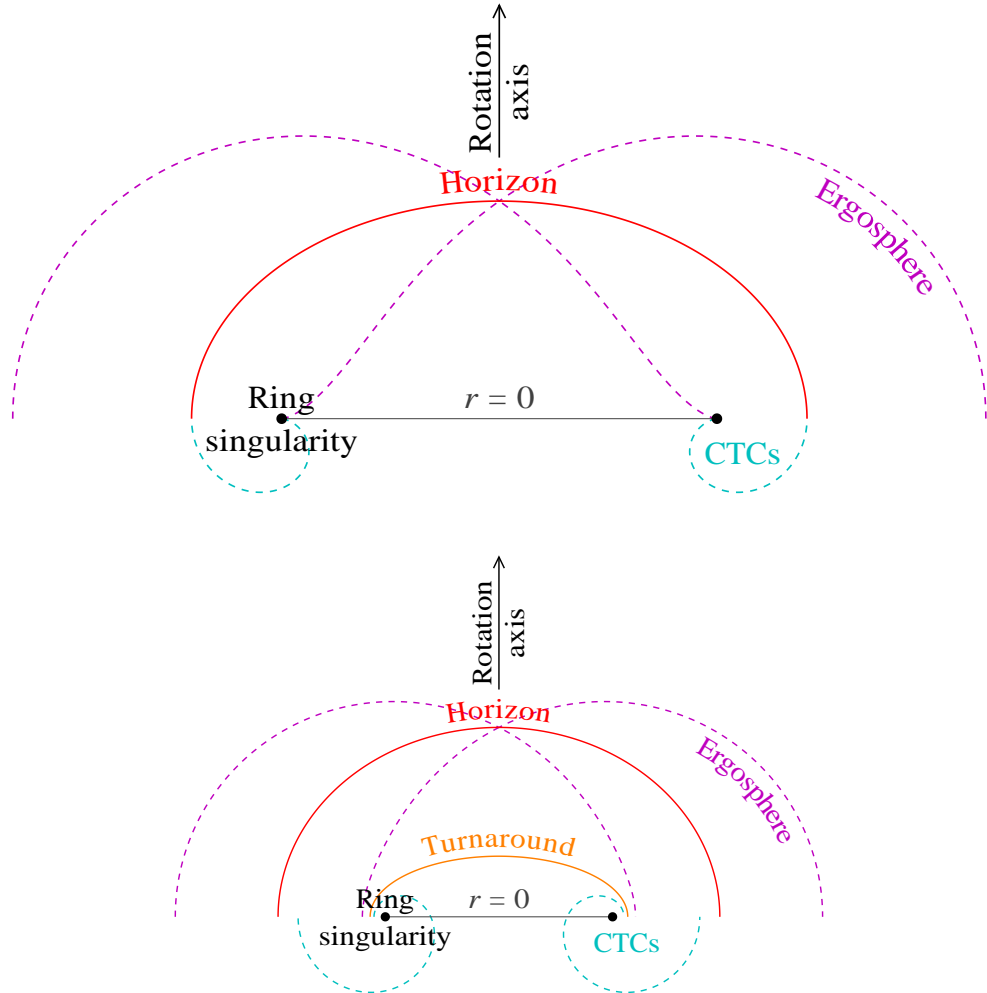


Figure 10: Geometry of (upper) an extremal ($a = 1$) Kerr black hole, and (lower) an extremal Kerr-Newman black hole with charge $Q = 0.8$ and spin parameter $a = 0.6$.